EVALUATION OF PREFORMANCE FOR A NOVEL SIDE STREAM ENHANCED BIOLOGICAL PHOPSHPORUS REMOVAL CONFIGURATION AT A FULL-SCALE WASTEWATER TREATMENT PLANT

by

Kurt Carson

B.A., University of Colorado, 2009

A thesis submitted to the

Faculty of the Graduate School of the

University of Colorado in partial fulfillment

of the requirement for the degree of

Master of Science

Department of Civil, Environmental and Architectural Engineering

2012

This thesis entitled:
Evaluation of a Novel Side Stream Enhanced Biological Phosphorus Removal Configuration at a Full-Scale Wastewater Treatment Plant
Written by Kurt Andrew Carson
Has been approved for the Department of Civil, Environmental and Architectural Engineering

Dr. Joann Silverstein

James McQuarrie

Date 8/13/2012 .

The final copy of this thesis has been examined by the signatories, and we Find that both the content and form meet acceptable presentation standards Of scholarly work in the above mentioned discipline.

Carson, Kurt Andrew (M.S., Civil, Environmental and Architectural Engineering)

Evaluation of a Novel Side Stream Enhanced Biological Phosphorus Removal Configuration at a Full-Scale Wastewater Treatment Plant

Thesis directed by Professor Joann Silverstein

Many wastewater treatment plants (WWTP) in the United States are facing new and previously unregulated phosphorus discharge limits from government regulatory agencies. While conventional enhanced biological phosphorus removal (EBPR) design criteria is proven and easily incorporated into the construction of new WWTPs, pre-existing WWTP often have site and capital constraints that make conventional EBPR designs costly and difficult to implement. A full-scale novel side stream EBPR configuration was implemented and tested at Metro Wastewater Reclamation District's Robert W. Hite Treatment Facility in Denver, Colorado. By design, the side stream EBPR configuration shows advantage over mainstream EBPR configurations because the integrity of the anaerobic zone is protected from downstream electron acceptors and high suspended solids concentrations in the side stream reactor allows for a minimal footprint. The results from an eight month 106 MGD demonstration showed excellent EBPR process performance. The attributes that make this EBPR configuration unique are the carbon requirement for anaerobic volatile fatty acid uptake is satisfied with gravity thickener overflow and the configuration required minimal construction and modifications to existing infrastructure for implementation. During the proof-of-concept test phase the novel EBPR configuration produced an average effluent total phosphorus concentration equal to 0.58 mg-P/L and a phosphate concentration of 0.11 mg-P/L. Evaluation of the novel EBPR configuration involved a detailed characterization of the gravity thickener overflow and extensive phosphate profiling throughout the secondary treatment complex. The design of the side stream EBPR configuration, process considerations, results of the study and future design considerations are discussed.

Acknowledgments

I would like to jointly thank Liam Cavanaugh and James McQuarrie for their continual support and guidance of my work at Metro. Their extensive feedback and technical expertise helped further the development of my research project and me as a professional. I would also like to thank my advisor, Dr. Joann Silverstein, for her input and sparking my interest in, and further study of, wastewater treatment.

I would also like to extend appreciation to Dr. Mark Hernandez for his guidance and service as my committee member. I would like to acknowledge Metro Wastewater Reclamation District for selecting me as a temporary O&M engineer and for funding this research. Additionally, I would like to thank all of the MWRD's staff that assisted me in this research, including but not limited to Tanya Bayha and Craig Barnes.

Most importantly, I would like to thank my mother, Christina Hansell. I am beyond grateful for her encouragement and unwavering support throughout my upbringing and during my studies at CU Boulder. Without her assistance none of this would have been achievable.

CONTENTS

TABLES

FIGURES

EQUATIONS

CHAPTER I

INTRODUCTION

Metro Wastewater Reclamation District Robert W. Hite Treatment Facility

Metro Wastewater Reclamation District's (MWRD) Robert W. Hite Treatment Facility (RWHTF) is a 220 MGD rated wastewater treatment facility, located in Denver, CO. RWHTF serves 1.7 million people in and around the Denver metropolitan area and is the largest wastewater treatment facility in the Rocky Mountain West region, treating a daily average of 140 MGD. The treated wastewater from RWHTF is suitable for agriculture, aquatic life, industrial use, water supply and recreation. MWRD's mission is "To provide wastewater transmission and treatment services to Metro District ratepayers in an efficient, cost-effective manner while continuing to meet all statutory and regulatory requirements". Over the years MWRD was earn many prestigious awards including 13 consecutive Platinum Awards from the National Association of Clean Water Agencies for no numerical permit violations, US EPA Operations and Maintenance Award for being the best operated and maintained wastewater treatment plant in the USA, and a certificate for Environmental Management System of Biosolids from the National Biosolids Partnership. These accolades give credence to MWRD staff's focus on continually identifying and promoting the most fiscally responsible means of providing reliable, sustainable and environmentally responsible wastewater treatment.

The source of wastewater that RWHTF treats originates from a combination of municipal, industrial and combined sewer storm water runoff. The effluent from RWHTF is discharged into the South Platte River and a portion is used as influent for

Denver Water's Reuse Plant. RWHTF's treatment processes consist of primary treatment, secondary treatment with biological nutrient removal (BNR) capabilities, and anaerobic digestion with cogeneration of methane for electricity production. The primary treatment process is a conventional solids separation but the secondary treatment processes at RWHTF are composed of a split south (SSEC) and north (NSEC) secondary treatment complexes.

Historically, the SSEC was designed and operated as a high purity oxygen treatment process for only biochemical oxygen demand (BOD) removal. However, the SSEC is currently undergoing large scale construction upgrades that will replace the high purity oxygen system with a Modified Ludzack-Ettinger (MLE) treatment process that will include a conventional mainstream enhanced biological phosphorus removal treatment (EBPR) configuration. The EBPR configuration implemented in the SSEC upgrades are based off conventional mainstream design criteria where primary effluent is conveyed to anaerobic zones at the beginning of each MLE treatment processes. When the construction upgrades are complete, the SSEC with have full BNR capacity to treat both nitrogen and phosphorus. The NSEC was designed and is operated as a MLE treatment process that currently only has the BNR capacity to remove nitrogen.

Within the near future, MWRD will have to comply with new effluent phosphorus discharge limits. It is anticipated that the new phosphorus discharge regulations could have final long term total phosphorus (TP) limit as low as 0.1 mg-P/L, with initial interim compliance TP limit of 1.0 mg-P/L. To meet the future TP discharge limits multiple phosphorus removal technology must be used. Implementation of an EBPR configuration will be a key wastewater unit process required to reduce the phosphate

concentrations in the effluent, which currently averages approximately 2.8 mg-P/L in the effluent which is equal to about 1500 kg-P/day.

Implementation of an EBPR configuration in the NSEC will necessitate new construction upgrades to the NSEC and/or a retroactive repurposing of existing infrastructure. New construction already underway in the SSEC plans to include a conventional EBPR configuration.

For implementation of an EBPR configuration in the NSEC, two distinct EBPR configurations were considered. The first EBPR configuration is a conventional mainstream approach (identical to the EBPR configuration under construction in the SSEC) where primary clarifier effluent is conveyed to anaerobic zones located at the head of each MLE train. This conventional configuration relies on standard EBPR design criteria.

Some of the requirements of retroactively adding this conventional EBPR configuration to the NSEC are that the anoxic zones at the head of each MLE train must be converted to anaerobic zones and two additional MLE trains would need to be constructed to replace the loss MLE capacity from the anoxic zone to anaerobic zone conversion. Another significant requirement of this EBPR configuration, is that addition of supplemental carbon (acetic acid) would be required to fully de-nitrify the nitrate rich Centrate and RAS Re-aeration Basin (CaRRB) effluent which is located upstream of the dedicated anaerobic zones and acetic acid would need to be fed to the anaerobic zones to satisfy the VFA requirement for the EBPR process. The initial planning-level estimated cost of this conventional approach would be 88.8 million dollars in capital construction cost and an annual cost of supplemental carbon between 1.6 and 3.2 million dollars. See

figure 1, below, for a diagram of the conventional EBPR configuration that is being considered for the NSEC.

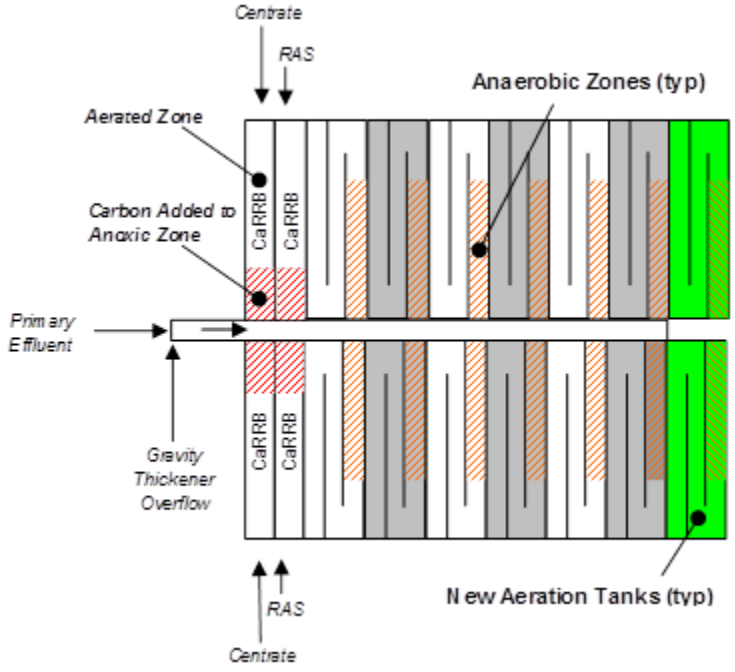

Figure 1. The conventional EBPR process configuration proposed for the NSEC. Note the red boxes indicate the repurposed anoxic zones which are converted into anaerobic zones and the green boxes indicate the new MLE trains that would be constructed.

An alternative novel EBPR configuration was envisioned that may provide significant cost savings over the conventional EBPR configuration being considered. This novel EBPR configuration would not require the construction or modification of existing MLE trains. Instead, the novel EBPR configuration would consist of a side stream approach where two of the four existing CaRRB reactors would be repurposed into anaerobic RAS reactors; gravity thickener overflow (GTO) and RAS would be conveyed to the anaerobic RAS reactors to satisfy the anaerobic VFA uptake requirement of EBPR. This configuration eliminates the need for supplemental carbon sources because the side stream EBPR process is isolated from the nitrate rich CaRRB effluent; therefore it is not important to fully de-nitrify the CaRRB effluent upstream of the MLE trains as in the

conventional EBPR configuration. In addition, this novel EBPR configuration does not need a supplemental carbon source for the VFA requirement of the EBPR process because the GTO can satisfy that requirement when conveyed to the anaerobic RAS reactor. This configuration is also unique in that the only modifications required for full scale implementation is the installation of six hydro-foil mixers with platforms in the anaerobic RAS reactor, piping from the gravity thickeners (GVT) to the anaerobic RAS reactor and a GTO pump. The cost of the modifications required to implement this EBPR configuration for an 8 month full-scale demonstration in the NSEC was approximately $255,000 and there is a small increase in O&M cost compared to standard operation without EBPR capacity. The increased operational cost from the novel EBPR configuration is related to extra electricity consumption from six additional two-horsepower mixers that would need to be installed in the anaerobic RAS reactor. See the diagram below for a diagram of the novel EBPR configuration in the NSEC.

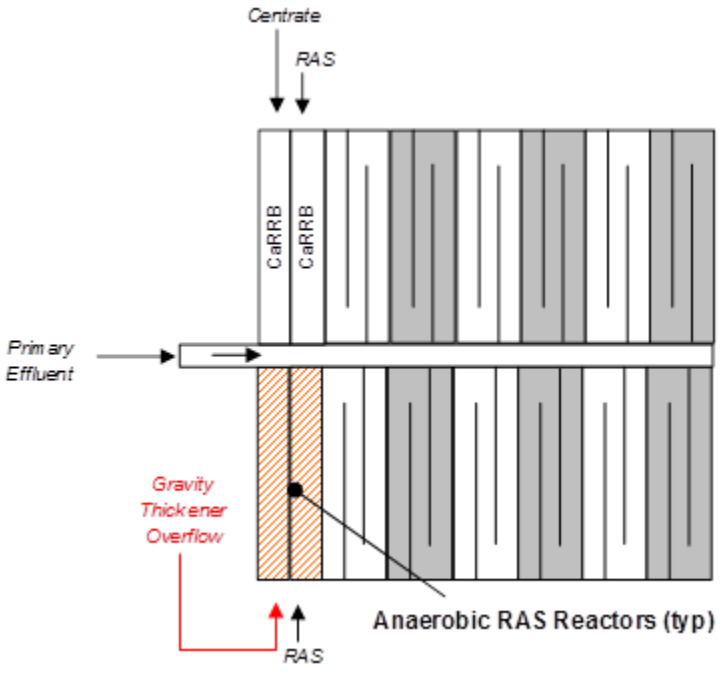

Figure 2. The novel EBPR configuration tested during the full-scale demonstration. Note the red dashes indicate the two repurposed CaRRB reactors converted into anaerobic RAS reactors.

Some of the other distinctive characteristics of the novel EBPR configuration are the high solids concentration in the anaerobic RAS reactor allows for a small anaerobic zone footprint compared to other mainstream configurations that utilize lower mixed liquor suspended solids (MLSS) concentration in the anaerobic zones. Also, the composition of the carbon substrate in the GTO not only includes volatile fatty acids (VFA), but also significant amounts of readily biodegradable chemical oxygen demand (rbCOD), slowly biodegradable chemical oxygen demand (sbCOD) and particulate organic matter. The diverse assemblage of carbon substrates conveyed to the anaerobic RAS reactor allows for multiple VFA formation pathways to arise while in the anaerobic RAS reactor in addition to the input of preformed VFAs originating from the gravity thickener overflow.

Initial investigations targeting a proof of concept for the novel EBPR configuration used Biowin and GPS-X model simulations. The model simulations predicted that the novel configuration could be a viable EBPR process in the NSEC when 100% of the GTO was conveyed to the anaerobic RAS reactor. These first results were promising and prompted further investigations of the novel EBPR configuration. See the figure below for GPS-X model simulation results showing that NSEC effluent TP could be reduced to 1.0 mg-P/L from the baseline 2.6 mg-P/L.

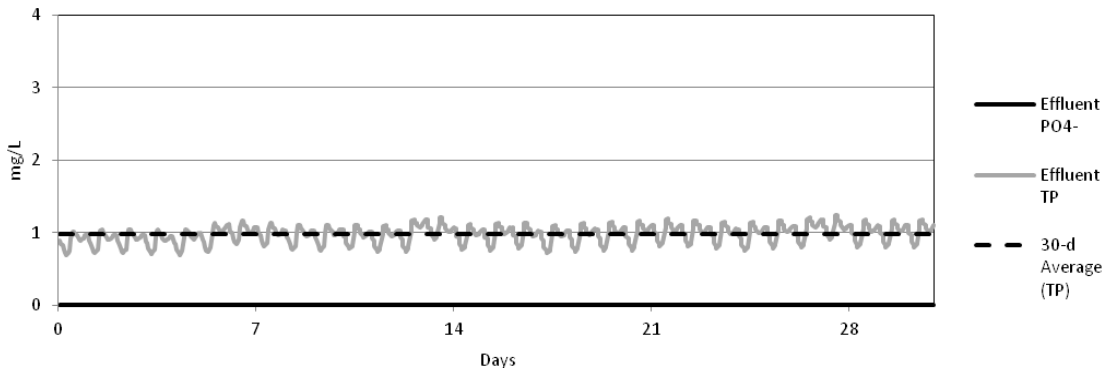

Figure 3. Dynamic GPS-X model simulation showing a reduction in NSEC effluent TP from 2.6 mg-P/L to 1.0 mg-P/L, when 100% of the GTO is conveyed to the anaerobic RAS reactors. TP concentration is on the left axis.

These model simulation results provide the initial evidence necessary to justify a more in-depth evaluation of the novel EBPR configuration and its feasibility. This promoted an 8 month full-scale demonstration (PAR 1171 - Enhanced Biological Phosphorus Removal) that was designed with the goal of determining if the novel EBPR configuration is viable and reliable enough to pursue as a permanent EBPR process configuration for the NSEC in the next facility plan.

PAR 1171 – Enhanced Biological Phosphorus Removal

The PAR 1171 full-scale demonstration was conducted between November 1st 2011 and June 30th 2012. The different time periods during the full-scale study are best referenced in relation to one of the six project phases, where the individual investigations were conducted. A brief description of each phase and a plot of effluent phosphate concentration during each phase follows, figure 4 below.

- **Phase I** - Phase I was conducted as the proof of concept and was used for collection of a baseline effluent phosphate dataset. November 1st 2011 – January 24th 2012.
- **Phase II -** During Phase II the gravity thickener sludge blankets were unintentionally varied as an adverse result of a plant wide control system upgrade. MWRD staff took advantage of this as a way to investigate the impacts that gravity thickener sludge blanket height has on VFA concentrations in the GTO and NSEC effluent phosphate concentration. January 25th 2012 – February 13th 2012.
- **Phase III -** During this phase poly-aluminum chloride was dosed to the NSEC complex to remedy sludge bulking issues that were unrelated to the PAR 1171 study. Phosphate precipitation in the NSEC, due to coagulant dosing, was examined. February 14th 2012 – March 31st 2012.
- **Phase IV -** RAS fermentation as a carbon source to support EBPR was investigated during this phase. April 1st 2012 – April 16th 2012.
- **Phase V** - This phase investigated the EBPR performance when 100% of the centrate was returned to the NSEC. April 17th 2012 – June 1st 2012.
- **Phase VI -** The goal of this phase to investigate the role that chemical addition (ferric chloride) plays in relation to the balance between phosphate loading to the NSEC and phosphate removal capacity and was a return to proof-of-concept performance. June 1st 2012 – June 30th 2012.

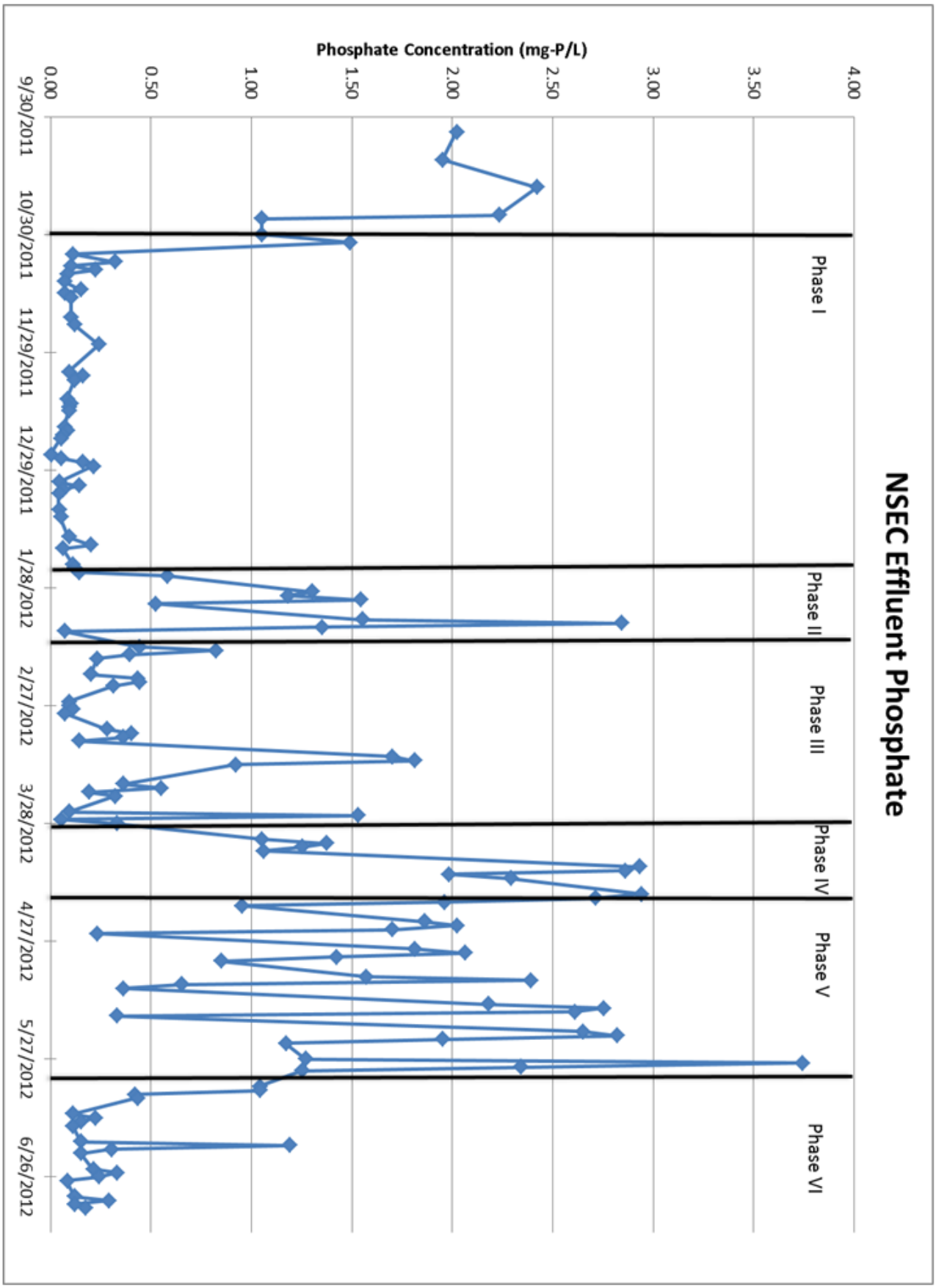

Figure 4. NSEC effluent phosphate concentration during the full-scale EBPR configuration testing for all study phases.

CHAPTER II

LITERATURE REVIEW

Enhanced Biological Phosphorus Removal

Enhanced biological phosphorus removal (EBPR) is biological process that selects for microbial heterotrophic phosphorus accumulating organisms (PAOs), which hyper-accumulate phosphorus in their biomass. Successful EBPR is a result of the proliferation of PAOs that are removed from the activated sludge process via proper sludge wasting. PAO proliferation relies on certain operational conditions that give PAOs a selective advantage and a selective disadvantage to other non-PAO heterotrophic microbes. The operational conditions that give PAOs their selective advantage is the presence of an anaerobic stage, void of electron acceptors, at the head of the secondary treatment process and an adequate supply of a readily biodegradable carbon source, typically in the form of volatile fatty acids (VFA).

In the anaerobic stage PAOs uptake the readily biodegradable substrate (VFA) and internally store it for latter growth in the aerobic zone. The PAOs internally store the VFA as polyhydroxyalkanoates (PHA) and polyhydroxybutyrate (PHB) (Fuhs and Chen, 1975). The PAO selective advantage is that PAOs are capable of storing readily biodegradable carbon in the anaerobic stage, while the carbon uptake of other heterotrophic microbes is inhibited by the anaerobic conditions. The anaerobic VFA uptake stage gives PAOs preferential access to readily biodegradable carbon substrates, which they later use as food for growth. This effectively gives PAOs the ability to access the best and highest energy yielding food source before other microorganisms and

subsequently allows PAOs to enrich their populations within the activated sludge system. The PAOs use energy during the anaerobic VFA uptake that comes from the breakdown of poly-phosphate molecules inside their cells, which when released increases the phosphate concentration in the bulk liquid (Fuhs and Chen, 1975). Phosphate is released during the anaerobic VFA uptake stage as a waste product from the intracellular energy transfer processes (Knowles, 1980). Adenosine triphosphate (ATP) is a multifunctional nucleoside which serves as an energy storage unit for cellular metabolism (Knowles, 1980). To utilize the stored energy reserves for cellular functions, an enzyme cleaves an ATP phosphate group converting it to diphosphate (ADP). Cleaving the phosphate group constitutes the breaking of covalent bonds and this process releases useful energy to the cell (Knowles, 1980). Magnesium and potassium ions are co-released with the phosphate during the anaerobic VFA uptake stage. Downstream in the aerobic stage, PAOs oxidize the internally stored PHA and PHB and rapidly grow. In the aerobic growth stage the PAOs uptake phosphate in excess of the phosphate mass released during anaerobic VFA uptake stage. See figure 5, below, for a figure describing the Fuhs & Chen theory of the mechanism of the EBPR process, note that HAc is the VFA source (Fuhs and Chen, 1975).

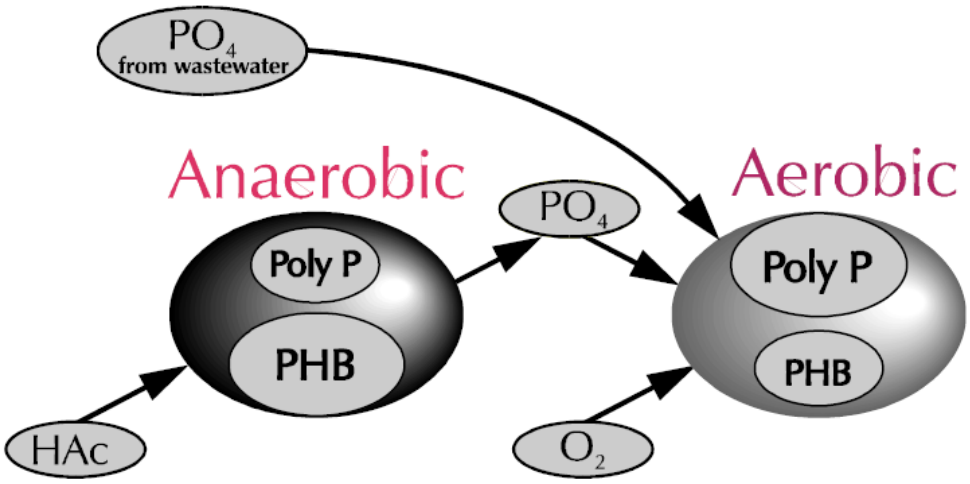

Figure 4. The Fuhs and Chen (1975) theory of EBPR mechanism.

The luxury uptake of phosphate into the biomass of the PAOs ultimately results in the net removal of phosphate from the liquid phase and hyper -accumulation of phosphate in the solid biomass. The EBPR process is completed when the phosphorus enriched biomass is removed from the activated sludge process through proper wasting.

Conventional EBPR Configurations

All EBPR configurations follow the same basic design of anaerobic, anoxic and aerobic zones. However, even though the principal design is the same there are many variations and modifications to the basic EBPR process that have produced the different EBPR configurations, which are generally recognized as conventional. Each conventional EBPR configuration has been altered to accomplish specific design goals, such as protection of the integrity of the anaerobic zone from electron acceptors, inclusion of a fermentation stage or differing levels of effluent nutrient concentrations (USEPA, 2009). The most commonly implemented conventional EBPR configurations are listed below.

- Pho-redox (A/O)
- 3 stage Pho-redox (A2/O)
- Modified Bardenpho
- University of Capetown (UCT) and Modified UCT (MUCT)
- Johannesburg (JHB) and Westbank
- Orange Water and Sewer Authority (OWASA)
- Hybrid chemical/biological processes

The performance of these EBPR configurations depends on many factors, some of which include; chemical additions, hydraulic and organic loading, recycle rates and return streams. When operated correctly, it is common that these EBPR configurations are capable of reducing effluent phosphate concentration below 1.0 mg-P/L. It has been observed that optimal operation of some EBPR configurations can produce ultra-low effluent phosphate concentrations to levels of about 0.1 mg-P/L (USEPA, 1993). See figures 5-10, below, for the basic flow diagrams of some the conventional EBPR configurations listed above (below figures adapted from USEPA, 2009).

A/O EBPR configuration

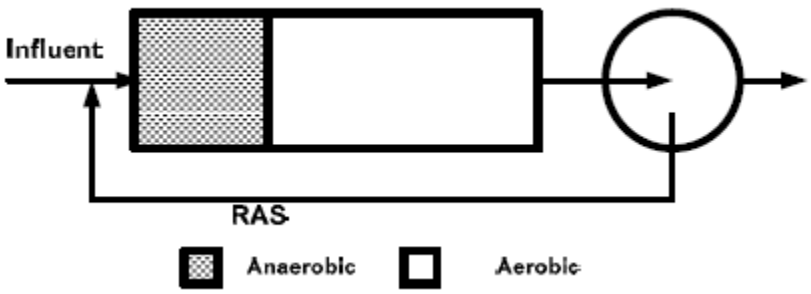

Figure 5. Typical flow diagram for Pho-redox (A/O) EBPR configuration.

A2/O EBPR configuration

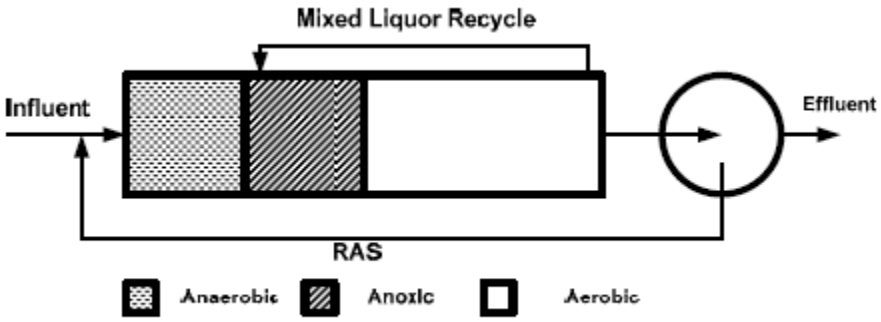

Figure 6. Typical flow diagram for 3 stage Pho-redox (A2/O) EBPR configuration.

UCT and MUCT EBPR configurations

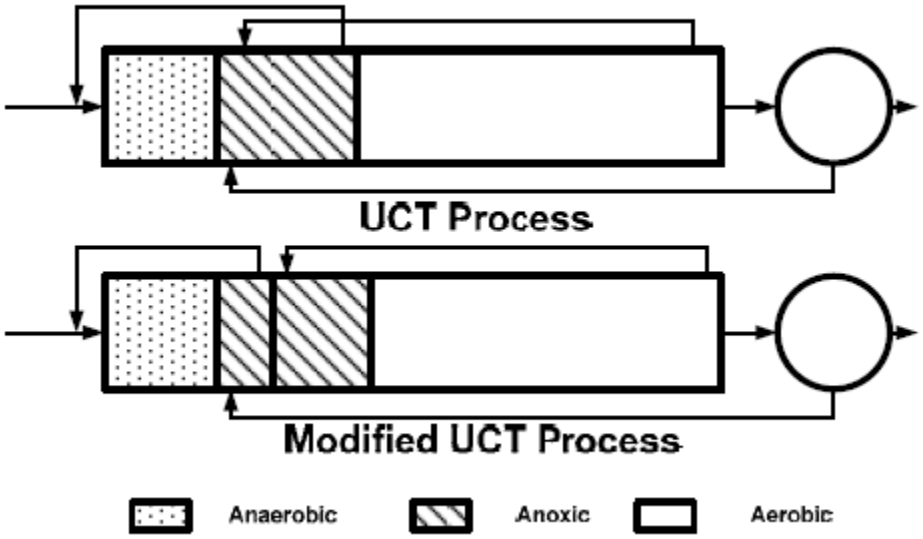

Figure 7. Typical flow diagrams of UCT and MUCT EBPR configurations.

JHB and Modifies JHB EBPR configurations

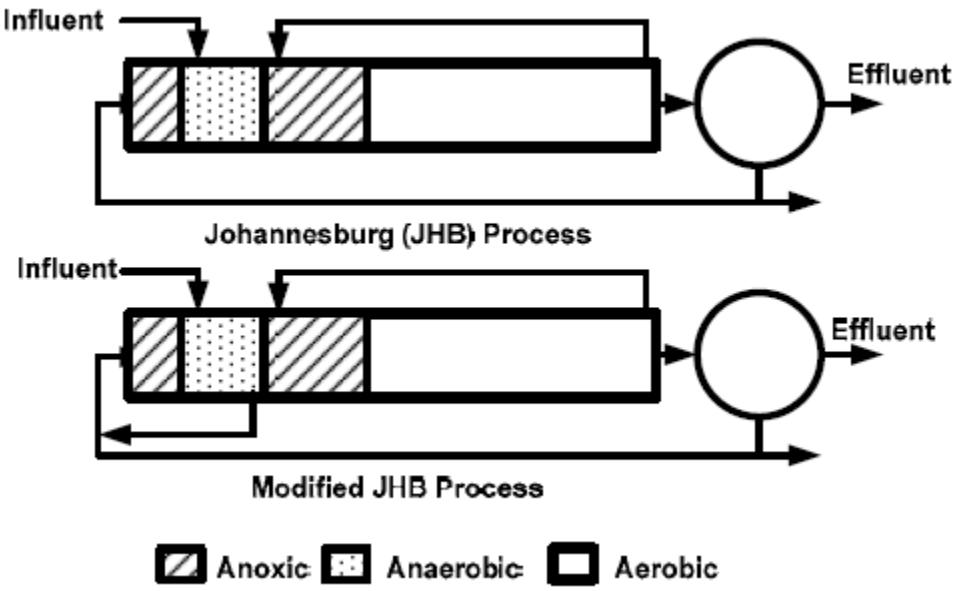

Figure 8. Typical flow diagram for JHB and Modified JHB EBPR configuration.

Westbank EBPR configuration

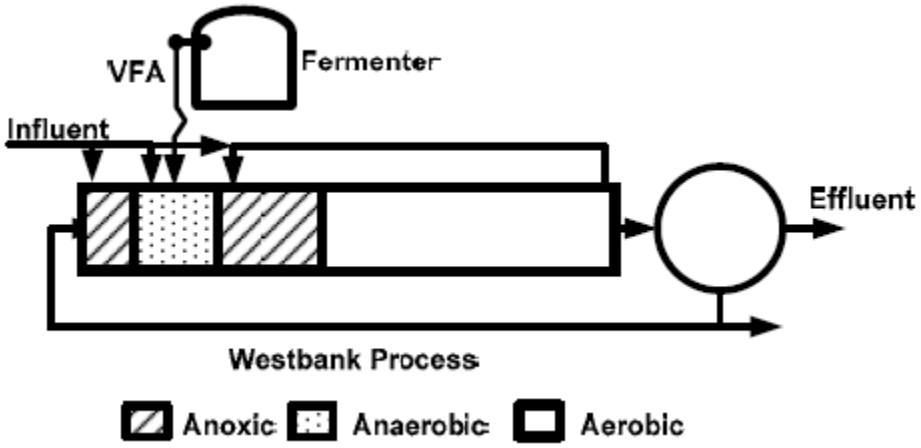

Figure 9. Typical flow diagram for Westbank EBPR configuration

OWASA EBPR configuration

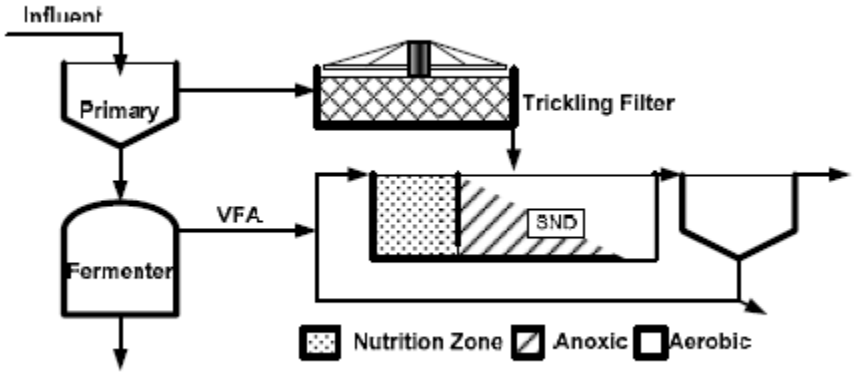

Figure 10. Typical flow diagram for OWASA EBPR configuration.

EBPR Operational and Design Considerations

Lots of research has been focused on identifying and understanding the factors that influence EBPR processes. The most important considerations that should be reviewed before implementing an EBPR configuration are listed below, followed by a brief description of their effects on the EBPR process (WEF and ASCE, 2003).

- Flow and load balancing
- Presence of electron acceptors in the anaerobic stage
- Temperature
- pH
- Secondary phosphate release
- Retention times (SRT and HRT)
- Anaerobic carbon requirement

Wastewater flows and nutrient loads vary due to daily diurnal water use patterns and due to irregular events such as storm water runoff. This non-steady pattern of flow and nutrient loading can have adverse effects on EBPR systems and can result in poor performance. Peaking events and sudden changes to nutrient loading should be avoided whenever possible. Equalization basins and/or nutrient sensors are useful to help balance

out flow and nutrient loading to EBPR systems (WEF and ASCE, 2009). To help balance nutrient loading, nutrient rich recycle streams, such as centrate, should be stored during times of high nutrient loading and fed during times of lower loading. Well balanced flow and loading patterns increase the stability of EBPR systems (WEF and ASCE, 2009).

Electron acceptors (oxygen and nitrate) should be minimized in the anaerobic zone. Non-PAO microorganisms that use oxygen or nitrates as electron acceptors will oxidize organic substrates (including rbCOD and VFA) in the anaerobic zone and reduce the VFA availability. Additionally nitrate can inhibit the fermentation of rbCOD to VFA because a many fermenters are facultative and can use nitrate as an electron acceptor to mineralize rbCOD instead of using the fermentation metabolic pathway (WEF and ASCE, 2009). The presence of nitrate and oxygen in the anaerobic zone increases VFA requirement for EBPR.

Temperature and pH influence the EBPR process. EBPR performance is impaired at temperatures above 28^{o}C (Bott et al., 2007) and EBPR is not possible at pH below 5.5 (Randall and Chapin, 1997). A report by WEF and ASCE (2006), found that when the pH falls below 6.9 EBPR process performance declines in efficiency.

Secondary phosphate release happens when PAOs are in anaerobic conditions in the absence of VFA. Phosphate is released to harness energy for cell maintain but during secondary release there is no associated VFA uptake and storage (Barnard, 1984). Without anaerobic VFA uptake, the PAOs are not able to uptake excess phosphate in downstream aerobic zones. According to the US EPA (2009), the three main sources of secondary phosphate release are, “In the anaerobic zone if the retention time is too high

and the VFA is depleted well within the required retention time. In the main anoxic zone when that runs out of nitrates. In the sludge blankets of the final clarifiers when the RAS rate is too low and sludge is not removed fast enough."

The minimum SRT required for good EBPR performance is 3 to 4 days (WEF and ASCE, 2006). The ratio of anaerobic HRT to aerobic HRT in an EBPR system is important. In the anaerobic stage, sufficient HRT must be available for the PAOs to uptake VFA and form PHA, however if the HRT is too long, then PAOs can undergo secondary release after the VFA is exhausted. An optimization study (Neethling et al., 2005) determined that a ratio of aerobic zone HRT to anaerobic zone HRT in the range of 3 to 4 produced the best phosphate removal.

Anaerobic carbon requirement for EBPR

Frequently, EBPR processes are restricted by carbon availability. The carbon requirement depends on the balance between influent phosphate load and amount of VFA available during the anaerobic uptake stage. Phosphate uptake capacity in the aerobic zone is directly related to the amount of phosphate released in the anaerobic stage (Comeau et al. 1987). The initial release of phosphate allows the PAOs to harness stored energy reserves, which is used to anaerobically uptake VFA. Increased anaerobic VFA uptake increases the amount of phosphate initially released and ultimately increases the amount of phosphate removed during the aerobic stage. Similarly, insufficient VFA availability in the anaerobic VFA uptake stage results in a decreased anaerobic VFA uptake, which diminishes the downstream aerobic phosphate uptake capacity (Temmink

et al. 1996). For that reason, overall EBPR process performance is dependent of the availability of a sufficient carbon source during the anaerobic VFA uptake stage.

According to the literature, the most desirable species of VFA, useful to support EBPR process, are acetic and propionic acids (GonCalves, 1994; Skalsky and Daigger, 1995; Wentzel et al., 1989). These are the smallest molecular weight VFA species and most abundant end-products produced in municipal wastewater primary solids fermentation. In addition to acetic and propionic acid, butyric and valeric acids can also be a significant portion of the VFA species present as fermentation end-products. A study by Skalsky and Daigger (1995) found a relative composition of 38 - 41% acetic acid, 36 - 44% propionic acid, 9 - 16% butyric acid, and 5 - 10% valeric acid as the fermentation end-products in a full scale wastewater fermenter. This is in agreement with a study by Elefsionitis and Oldham (1991) which determined that acetic and propionic acids together compose up to 75 - 80% of total VFA end- products during fermentation of primary solids. See table 1, below, for the characteristics and COD equivalents of the most common VFA species present in wastewater fermentation processes (Rossle and Pretorius, 2001).

VFA characteristics and COD equivalents				
Common name	Formula		Molecular weight (g/mol)	COD equivalent (mg-COD /mg-VFA)
acetic acid	CH_3COOH	$C_2O_2H_4$	60.05	1.067
propionic acid	CH_3CH_2COOH	$C_3O_2H_6$	74.08	1.514
butyric acid	$CH_3(CH_2)_2COOH$	$C_4O_2H_8$	88.11	1.818
valeric acid	$CH_3(CH_2)_3COOH$	$C_5O_2H_{10}$	102.13	2.039
caproic acid	$CH_3(CH_2)_4COOH$	$C_6O_2H_{12}$	116.16	2.207

Table 1. VFA characteristics and COD equivalents. Adapted from Rossle and Pretorius, 2001.

Over the years, significant research efforts have focused on determining the carbon to phosphorus ratio required in the anaerobic VFA uptake stage to facilitate adequate

phosphate removal. By convention the ratio is based on measurements of mg COD to mg-P, where the P mass is calculated from soluble phosphate in the influent streams. The carbon is measured in COD, BOD, rbCOD and/or VFA, with rbCOD being the most accurate measure when theoretical ratios are compared to the observed phosphate removal. See table 2, below, for the reported minimum carbon to phosphorus ratio required in the anaerobic stage to promoted satisfactory phosphate removal in EBPR systems (WEF, 2010).

Minimum carbon to phosphorus requirement for EBPR	
Substrate measure	**Substrate : P ratio**
$cBOD_5$	20:1
$sBOD_5$	15:1
COD	45:1
VFA	7:1 to 10:1
rbCOD	15:1

Table 2. Minimum carbon to phosphorus ratio requirement for EBPR, note that these ratios refer to reactor influent and should account for recycle loads and removal in the primaries. Adapted from WEF, 2010.

Depending on desired level of phosphate removal, carbon may need to be added to meet effluent goals. The most common supplemental carbon source used to simulated EBPR systems is acetic acid addition directly to the anaerobic stage. Even though supplemental acetic acid addition is the most common approach to make up carbon deficits in the anaerobic stage, addition of non-VFA carbon sources have been shown to supply sufficient carbon required in the anaerobic stage and these non-VFA supplements have been able to achieve very low effluent phosphate concentrations (Thomas et al., 2003). The Thomas et al. (2003) study added molasses to an upstream fermenter, which was converted to VFA during the fermentation process and ultimately used as a carbon source latter in the anaerobic stage of their EBPR configuration. This study was able to reduce phosphate concentrations to approximately 0.1mg-P/L in their effluent using this approach.

Another approach that has been utilized to satisfy the VFA requirement without the addition of an external carbon source is sludge fermentation. Both primary and secondary sludge have been successfully fermented and used as the VFA source for EBPR processes. There are multiple sludge fermentation designs and operational schemes that can be used to increase VFA production, some of which are listed below (USEPA, 2009).

- Activated primary sedimentation basins
- Elutriation of primary clarifiers
- Elutriation of gravity thickeners
- Side stream RAS fermentation
- Increased SRT of sludge in gravity thickeners and use of supernant

The most important factor to consider, pertaining to sludge fermentation for VFA production with an EBPR system, is that sludge fermentation processes operate best with a high solids concentration and sufficiently long retention times to facility the fermentation reactions (USEPA, 2009).

CHAPTER III

NOVEL EBPR CONFIGURATION AND PROCESS CONSIDERATION

The implementation of the of the novel EBPR configuration for the PAR 1171 study required that two of the four existing CaRRB reactors be repurposed into anaerobic RAS reactors. By design, the CaRRB reactors used fine bubble diffusers on the first 60% of the bottom of the basins to mix the bulk liquid and keep solids suspended. The remaining 40% of the CaRRB reactors are for de-nitrification and have two existing platform mixers in the anoxic compartments. Since anaerobic conditions and solid suspension are a requirement of the anaerobic RAS reactor, platform mixers needed to be installed in the first 60% of the basins to replace the mixing function of the diffusers which were off-line in the anaerobic RAS reactor. The mixers installed (6 in total between to anaerobic RAS reactors) were intentionally designed to have low mixing energy to promote large MLSS flocculent particles in the reactor. The flow diagram for the novel EBPR configuration is below.

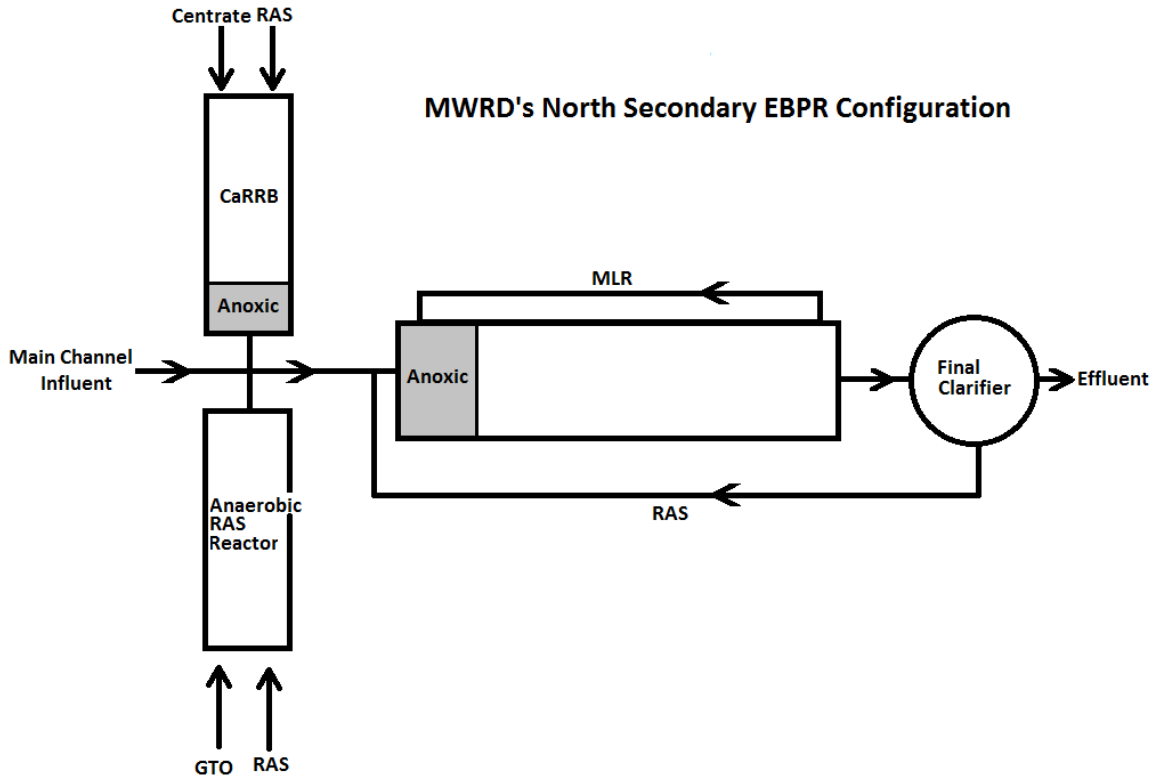

Figure 11. Novel EBPR configuration flow diagram implemented in the NSEC.

Other major modification necessary in the NSEC was the installation of a temporary piping from the gravity thickener overflow weir to the head of the two anaerobic RAS reactors. A gravity thickener overflow pump was also needed to convey the GTO to the anaerobic RAS reactor. The design criteria for anaerobic RAS reactor and mixer configuration are shown below in table 1 (Cavanaugh et al., 2012).

Criterion	Novel Side Stream EBPR Design	Conventional EBPR Design
Anaerobic RAS Reactor Volume	1.36 million gallons	4.9 million gallons
RAS Flow to Anaerobic Zone	20 mgd	100 mgd
Suspended Solids Concentration Anaerobic Zone	6000 mg/L	3000 mg/L
% of Anaerobic Reactor RAS Throughput (Total)	18.3%	100 %
GTO Flow to Each Reactor	5.30 mgd	N/A
Anaerobic Hydraulic Retention Time	1.1 - 1.30 hours	0.5 – 0.75 hours
Anaerobic Solids Retention Time	0.49 days	0.5 – 1.5 days
Hydrofoil Mixer Rotational Speed, n	27 rpm	40-125 rpm
Hydrofoil Mixer Velocity Gradient, G	46.5 s^{-1}	50-100 s^{-1}
Hydrofoil Mixer Power Number, Np	0.31	0.30
Hydrofoil Mixer Flow Number, Nq	0.53	0.50
Anaerobic carbon requirement (COD:P)	10:1 to 15:1	45:1
Anaerobic carbon requirement (VFA:P)	2:1 to 3:1	7:1 to 9:1
Anaerobic carbon requirement (rbCOD:P)	4:1 to 5:1	10:1 to 15:1

Table 3. Conventional design from WEF Manuel of Practice 8, 2010and Metcalf and Eddy, 2003. Initial anaerobic RAS reactor operational parameters and design criteria for the two repurposed CaRRB reactors. Figure adapted from Cavanaugh et al. 2012.

The total combined underflow rate from all the primary clarifiers ultimately determines the gravity thickener loading and subsequent gravity thickener overflow and underflow rates. The gravity thickener only thickens primary sludge from the primary clarifiers. There are no upstream additions of metal salts, secondary sludge or surfactants to the influent of the gravity thickener. Before the study began, the primary underflow

rates were modified from a density control set-point to a constant flow set point. These initial changes were done in an effort stabilize flow fluctuation to the gravity thickener. Historically, the primary underflow rates varied in response to daily solids loading patterns because the primary underflow pumping was controlled using a density set point of the primary sludge in the primary clarifiers. The historic density set point control for the primary underflow pumping rate was a thin sludge pumping operation with the control density of 1%. After the change to a constant underflow the flows to the anaerobic remained steady at about 3700 gallons per minute or about 5.3MGD to the anaerobic RAS reactor.

The operation of the gravity thickener was also altered before the start of the study. Historically, the underflow pumping from the gravity thickener was controlled at a density set point of about 4%. During the study period the gravity thickener underflow pumping was controlled manually in response to gravity thickener sludge blanket heights. Preliminary investigations before the study suggested that the concentration of rbCOD and VFA in the GTO had a proportional relationship to gravity thickener sludge blanket heights. The gravity thickener underflow pumping was varied in an effort to consistently maintain gravity thickener sludge blankets at approximately 8 feet.

The last operational change to the gravity thickener before the commencement of the study was than one of the four gravity thickeners had an elutriation loop installed. The elutriation loop consisted of a temporary four inch pipe that used a redundant gravity thickener underflow progressive cavity pump to redirect a small portion of the gravity thickener underflow back to the gravity thickener influent splitter box. In agreement with published literature on prefermenter design and operation with municipal sludge, this

initial elutriation scheme was implemented in an attempt to boost concentrations of VFA in the GTO (Ahm and Speece 2006, Ucisik and Henze 2008, Chanona et al 2006). The original elutriation pumping rate varied between 24 and 48 gallons per minute which corresponds to an elutriation rate less than 1% of influent loading.

Modifications were made to the MLE trains in the NSEC. Initially and for the majority of the study, the first two mixers in the A-pass of every MLE train were shutoff. These modifications were implemented to test whether additional anaerobic volume could be obtained through the short-circuiting of the nitrate rich mixed liquor return (MLR) and through dead zones in the bottom of the tanks. During the study, monitoring was conducted to evaluate the anaerobic conditions in the unmixed compartments, impacts on de-nitrification, solids stratification and any additional anaerobic phosphate release. The results of these monitoring efforts are included in latter chapters.

CHAPTER IV

Gravity Thickener Overflow COD Partitioning to Anaerobic PO4 Release

INTRODUCTION

The GTO is composed of a diverse assemblage of different carbon substrate types that can be used by microorganisms for food. These broad carbon substrate types present in the GTO are best referenced in relation to COD characterization categories. The main generally recognized COD fractions used in wastewater characterization are soluble COD, colloidal COD and particulate COD. From an economic standpoint, there needs to be an efficient balance between the gravity thickener carbon conveyed to the anaerobic RAS reactor and the gravity thickener carbon sent to anaerobic digestion and cogeneration. The carbon flow to the anaerobic RAS reactor is essential for good EBPR process performance however, the carbon flow to anaerobic digestion process is critical for cogeneration of electricity from methane production. The literature states that only a small fraction of carbon is useful for PAOs during the anaerobic phase of EBPR processes, however in comparison, all organic carbon is useful in anaerobic digestion and cogeneration processes. The economic tradeoff is that sufficient loading of a proper carbon substrate needs to be satisfied in the anaerobic RAS reactor for good EBPR process performance but all excess carbon loading or carbon loading of an unsuitable type is wasted in relation to EBPR processes. The excess or wasted carbon sent to the anaerobic RAS reactor will not be fully capitalized on in cogeneration as secondary sludge and therefore this represents great operational inefficiencies. These inefficiencies can be diminished by operating the gravity thickener in a manner that reduces excess and

wasted carbon sent to the anaerobic RAS reactor, while still satisfying the carbon requirements of the EBPR process. Proper gravity thickener operation will maximize the worth of gravity thickener carbon.

By design and conventional practice, a gravity thickener is intended to be a physical solids separation process. In the novel EBPR configuration being tested, the gravity thickener is adapted to a duel role of being utilized as a carbon source for the anaerobic RAS reactor and solids separation. This dual functionality raises an important question about the proper operation of the gravity thickener to achieve desired results. Of importance is which fraction of the GTO carbon is most useful in the anaerobic RAS reactor to facilitate anaerobic phosphate release. The answer to the former question is useful from an operational standpoint to be able to promote good EBPR performance while not wasting carbon.

Experimental Design

A bench scale experiment was designed to investigate the relative contribution that soluble COD, colloidal COD and particulate COD has in relation to useful anaerobic phosphate release. The experimental design aimed at emulating the full scale conditions of the anaerobic RAS reactor, RAS and GTO were combined in a ratio equal to full-scale operation and duration of the experiment was representative of the full-scale anaerobic RAS reactor hydraulic residence time (HRT). The soluble COD fraction of GTO was isolated by flocculating and filtering colloidal and particulate substances from a fresh GTO sample. The colloidal fraction of the GTO was calculated as the difference between the soluble GTO sample and another GTO sample from the same batch that was only

filtered. The particulate fraction of the GTO was calculated as the difference between a raw GTO sample and a filtered GTO sample from the same batch.

Methodology

The bench reactor setup and experimental equipment consisted of three 1L containers, 3 stir plates, 3 magnetic stir bars, a timer, parafilm used to seal the batch reactors, 3 - 25mL pipettes and 30 flip-mate 0.45uM glass fiber filter single use vacuum filters apparatuses. A HACH DR 3900 spectrophotometer was used for phosphate analysis.

4L of fresh RAS and 3L of fresh GTO were collected immediately before the experiment. The 3L of fresh GTO was well shaken and then split into equal 1L portions. One GTO portion was filtered through a 0.45uM glass fiber filter and the filtrate was set aside, this filtered portion of GTO is referred to as “filtered GTO”. Another 1L portion of GTO was flocculated with aluminum sulfate and after a 5 minute wait for the flocculated particles to settled the supernatant was removed and filtered through a 0.45uM glass fiber filter. This filtrate was also set aside and this portion of GTO is referred to as “floc filtered GTO”. The last portion of GTO was not altered and is referred to as “raw GTO”.

210mL of “filtered GTO” was combined with 790mL of fresh RAS in a 1L container containing a magnetic stir bar. The time was recorded and the container was immediately sealed with parafilm and placed on a stir plate set to low. The mixing in the container was adjusted to the minimum setting to keep the stir bar rotating and solids suspended. The same procedure was immediately repeated with “floc filtered GTO” and “raw GTO”, combining them with fresh RAS in there owe dedicated containers.

At predetermined time steps of 5, 10, 15, 20, 25, 30, 45, 60, 75 and 90 minutes, 25mL aliquots of sample were withdrawn from each sealed reactor with a pipette. The aliquots were immediately filtered through a 0.45uM glass fiber filter, labeled and set aside for later phosphate analysis.

The initial phosphate concentration of the RAS, filtered GTO, floc filtered GTO and raw GTO were determined. The COD concentration was determined for filtered GTO, floc filtered GTO and raw GTO from the leftover volume not added to the batch reactor.

The phosphate analysis was conducted according to HACH method number 8114 which is EPA approved for wastewater analysis. The COD analysis was conducted by the Technical Services Laboratory according to standard methods (1998).

RESULTS

Soluble COD fractions in the GTO contribute greater than 90% of the anaerobic phosphate release observed in the bench scale reactor. Colloidal COD fractions in the GTO contribute about 4% of the ultimate anaerobic phosphate release observed in the bench scale reactor. Particulate COD fractions in the GTO contribute about 4% of the ultimate anaerobic phosphate release observed in the bench scale reactor. See figure 13, below, for the complete anaerobic release profiles of each additive COD fraction.

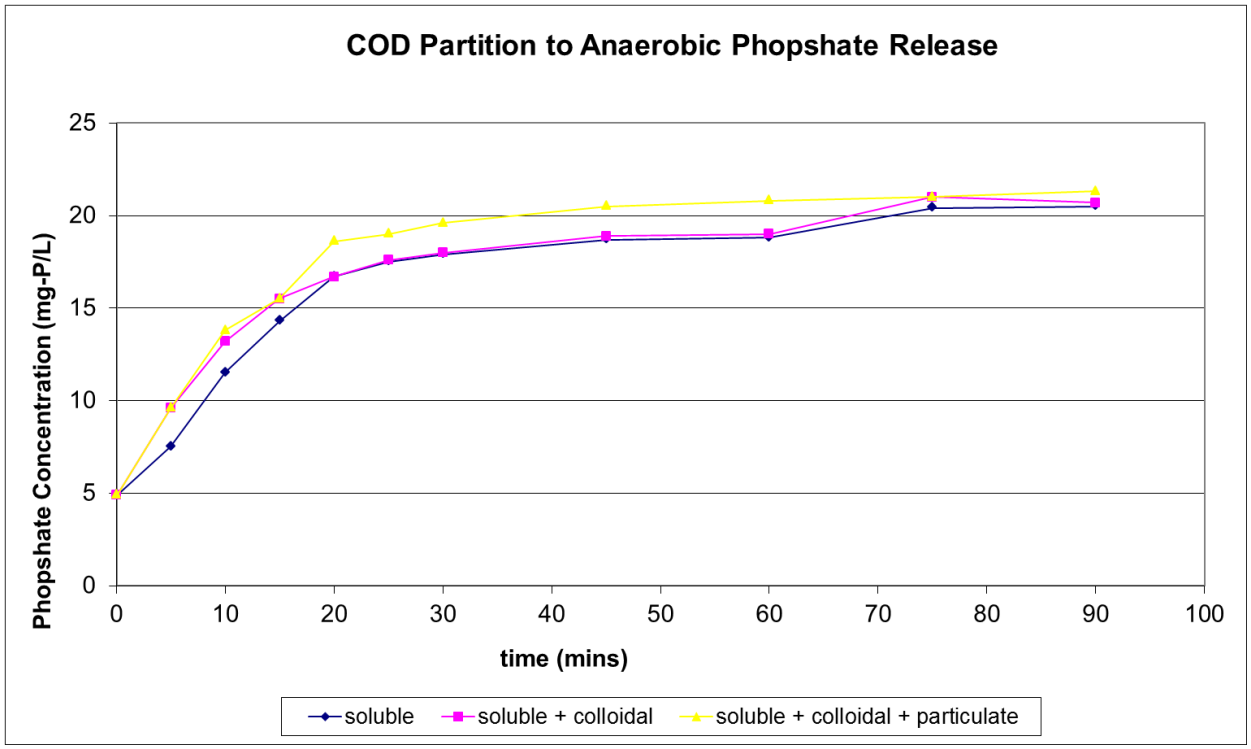

Figure 12. This figure shows the anaerobic phosphate release profiles for a bench scale reactor that best as possible emulates the full scale anaerobic RAS reactor. The different series indicate the additive contribution of the different COD fractions in the GTO.

Soluble COD is the dominant COD fraction of the total COD in the GTO which is equal to about 45% of total COD. Colloidal COD and particulate COD contribution are approximately equal at about 27-28% each of the total COD in the GTO. See table 4, below, for a summary of COD partitioning and contribution to phosphate release

COD partition in GTO	% contribution to PO4 release
soluble COD = 44.8%	91.1
collidial COD = 26.9%	4.4
particulate COD = 28.3%	4.5

Table 4. This table shows the percentage of total COD that each COD fraction represents in the GTO and the relative contribution that the individual fractions have on anaerobic phosphate release.

DISCUSSION

It is important to understand which COD fraction of the GTO contributes to anaerobic phosphate release. The three GTO fractions tested in the bench scale COD partition experiment were “filtered GTO”, “floc filtered GTO” and “raw GTO”. The floc filtered GTO sample only contains the soluble COD fraction that is present in GTO, due to the flocculation and filtering process. The filtered GTO sample only contains soluble and a portion of the colloidal COD fraction that is smaller than 0.45uM threshold. The raw GTO sample contains all the COD fractions present in GTO, which are soluble COD, colloidal COD and particulate COD.

Even though colloidal COD and particulate COD together constitute more than half of the COD being conveyed to the anaerobic RAS reactor, these COD partitions hardly contribute to anaerobic phosphate release. Soluble COD is responsible for more than 91% of the observed phosphate release in the anaerobic RAS reactor. This observation is in agreement with the literature and suggests that soluble COD is the most useful form of carbon substrate in the GTO in regards to EBPR processes.

The data suggests that the gravity thickener should be operated to maximize solids capture because the solid COD is not directly useful for EBPR processes in the anaerobic RAS reactor. All the particulate COD conveyed to the anaerobic RAS reactor represents excess wasted carbon because it does not support useful anaerobic phosphate release. Operating the gravity thickener to maximize solids capture while still providing sufficient VFA and rbCOD in the GTO to the anaerobic RAS reactor may be problematic in practice. Increased sludge blanket depths in the gravity thickener increases the rbCOD

and VFA concentration in the GTO, which is desirable for from an anaerobic carbon requirement perspective. However, increased sludge blankets in the gravity thickener also increases the likely hood of sludge blankets floating and solids overflowing into the gravity thickener weir. When this happens, excessive solids and carbon are being conveyed to the anaerobic RAS reactor which is wasted from a methane production and EBPR standpoint. When considering the effects that increased sludge blankets in the gravity thickener has on both solids capture and carbon concentrations in the GTO, it seems that it would be best to operate the gravity thickener in a way that maximizes rbCOD and VFA in the GTO because it is more important to satisfy the anaerobic carbon requirement than to worry about a small amount of wasted particulate carbon in the GTO. Even though some particulate carbon is being wasted the vast majority of solids in the gravity thickener are being sent to the anaerobic digestion process. The small amount of particulate carbon sent to the anaerobic RAS reactor is the associated cost of using GTO as the sole carbon to support EBPR in this novel configuration.

CHAPTER V

Gravity Thickener Overflow Characterization

Introduction

The gravity thickener at MWRD only thickens primary sludge from the primary clarifier underflow; the influent to the gravity thickener does not include any secondary sludge, metal salts or surfactants. Arguably, the gravity thickener could be considered one of the most important unit processes in the novel EBPR configuration required to get good phosphate removal. The initial GPS-X model simulations predicted that the EBPR configuration would not be able reduce TP below 1.0 mg-P/L without conveying 100% of the GTO to the anaerobic RAS reactor to fulfill the carbon requirement of the anaerobic VFA uptake phase. See GPS-X model dynamic simulation below for a scenario where only 50% of the GTO is conveyed to the anaerobic RAS reactor and average effluent TP is 1.2 mg-P/L, also note the large unstable fluctuations in effluent TP.

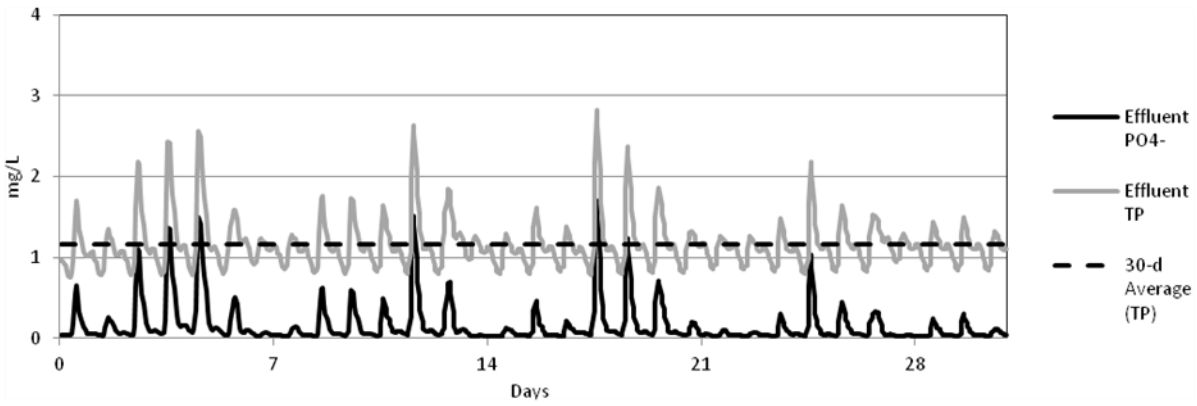

Figure 13. GPS-X dynamic simulation of effluent TP in a scenario where only 50% of GTO is conveyed to anaerobic RAS reactor.

Very quickly it became clear that it is important to characterize the carbon loading in the GTO to the anaerobic RAS reactor to understand the stability of the EBPR configuration and help identify modifications that could assist in the optimization of the

operation of gravity thickener as the sole carbon source for the novel EBPR configuration. Another observation that emphasized the importance of understanding the carbon loading in the GTO was that preliminary investigations examining the concentration of rbCOD and VFA in the GTO showed variability between grab samples taken on different days and between grab samples taken at the same time but on different individual gravity thickener overflow weirs. These initial observations raised many questions, some of which are listed below:

- What is the minimum, maximum and average daily carbon loading?
- How does the carbon loading in the GTO vary over the course of a day, or week or seasonally?
- What impact does the gravity thickener elutriation loop have on carbon loading?
- What impact do the sludge blanket heights in the gravity thickeners have on carbon loading?
- How does the underflow pumping from the primary clarifiers impact carbon loading in the GTO?
- What is the speciation of the carbon in the overflow?

In an attempt to answer the above questions and to gain insight into the role that the gravity thickener plays in relation to carbon loading to the anaerobic RAS reactor, multiple sampling campaigns was conducted over the course of the study to characterize the GTO. These sampling efforts include grab sampling, composite sampling and multiple diurnal sampling efforts.

Methodology

GTO samples were collected via grab samples in the gravity thickener overflow weir. The time of collection was recorded. To characterize the diurnal pattern of the

GTO, an auto-sampler was used to collect 1L samples from the overflow weir every two hour for up to 48 consecutive hours. Historically and throughout the study there have been 24hr composite auto-samplers installed in each individually gravity thickener overflow weir and a combined auto-sampler in the GVT underflow sludge. Samples were collected using the previously installed autosamplers and data was retrieved from the historical data sets previously recorded. The samples were analyzed for VFA, COD, BOD, rbCOD and TSS according to standard methods (Standard Methods 1998). The VFA analysis was conducted by the Technical Services Laboratory using a gas chromatography/mass spectrophotometry method.

Results

The table below summarizes the daily carbon loading to the anaerobic RAS reactor in each respective phase of the study, note that the observed range of average daily concentrations remain constant during periods of constant gravity thickener operation. The carbon loading increases in Phase V and Phase VI because flow increases to the GTO during those respective phases.

	VFA loading (kg-COD/day)	rbCOD (kg-COD/day)	COD (kg-COD/day)	BOD (kg-COD/day)
phase 1	3524	6445	18150	11480
phase 2	Unknown	Unknown	Unknown	Unknown
phase 3	3524	6445	18150	11480
phase 4	0	0	0	0
phase 5	4564	8346	23504.85	14867
phase 6	4300	7862	22113	14005

Table 5. Show the average daily GTO carbon loading to the anaerobic RAS reactor in each respective study phase

Table 6, below, shows the average daily carbon concentrations in the GTO. The daily average concentration were calculated using hourly concentrations data from four different diurnal carbon sampling datasets where samples were taken every two hours for the entirety of the day.

Average daily GTO concentration (mg-COD/L)			
VFA	rbCOD	BOD	COD
175	320	570	901

Table 6. Average daily GTO carbon concentrations

Over the course of a couple hours the concentrations of the different species of carbon in the GTO varied by almost a factor of three. Figure 15, below, shows the hourly variation of VFA in the GTO over the course of two consecutive days. The maximum VFA concentration during this period was 285 mg-COD/L and the minimum was 109 mg-COD/L. All the diurnal VFA concentration patterns had this same general shape and range of values. It is important to mention that the VFA concentration in the GTO is highest during the day around noon and decreases to a minimum concentration at night. The timing of the observed daily peak VFA concentration in the GTO during all diurnal carbon datasets is approximately noon and the observed minimum VFA concentrations are all about the same time at night which is approximately between midnight and 6am.

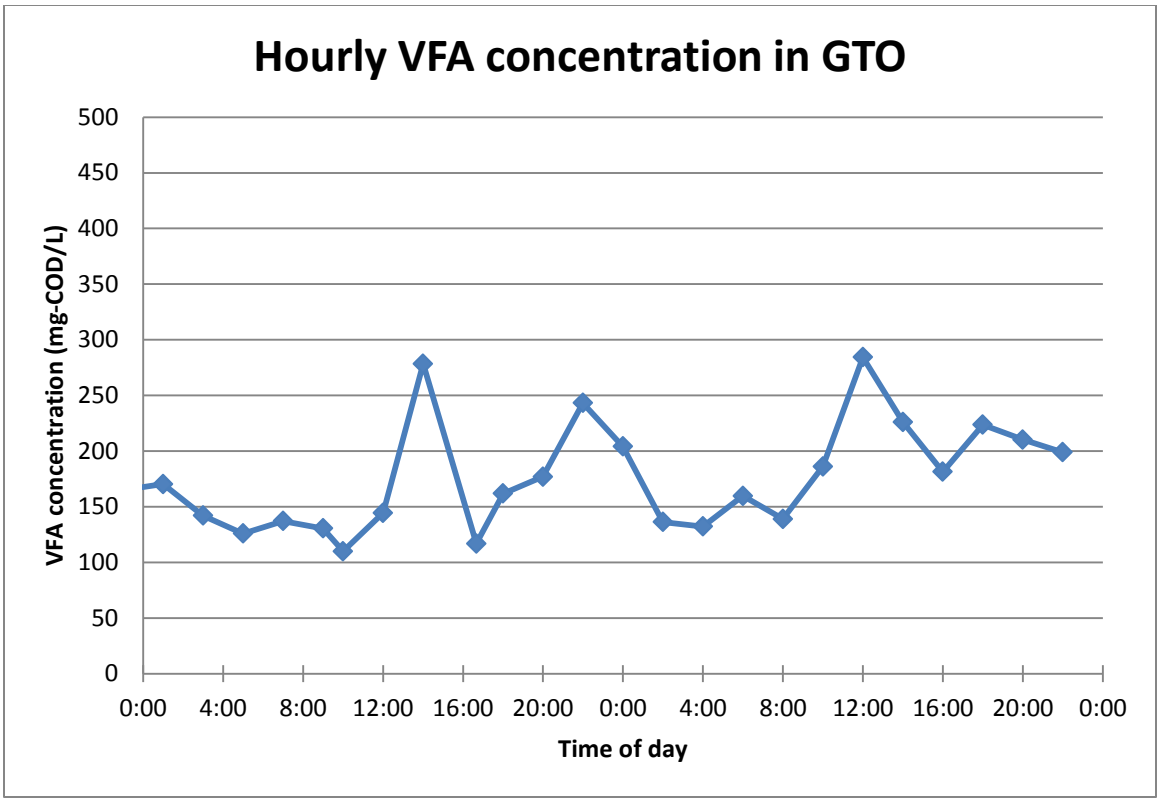

Figure 14. VFA concentration variation in the GTO over the course of two consecutive days.

Figure 16, below, shows the hourly rbCOD concentration in the GTO. The maximum observed rbCOD concentration during the diurnal sampling is 460 mg-COD/L and the minimum concentration observed is 281 mg-COD/L. All the diurnal rbCOD concentration patterns had this same general shape and range of values. Note that daily timing of the rbCOD peak concentration and rbCOD minimum concentrations shows the same general pattern as the VFA data. The daily timing of peak rbCOD concentrations in the GTO occurs at approximately noon every day and the daily timing of minimum rbCOD concentration in the GTO is occurs between midnight to 6am every day. This same general pattern of daily maximum and minimum rbCOD concentration is consistent in all diurnal rbCOD diurnal datasets collected.

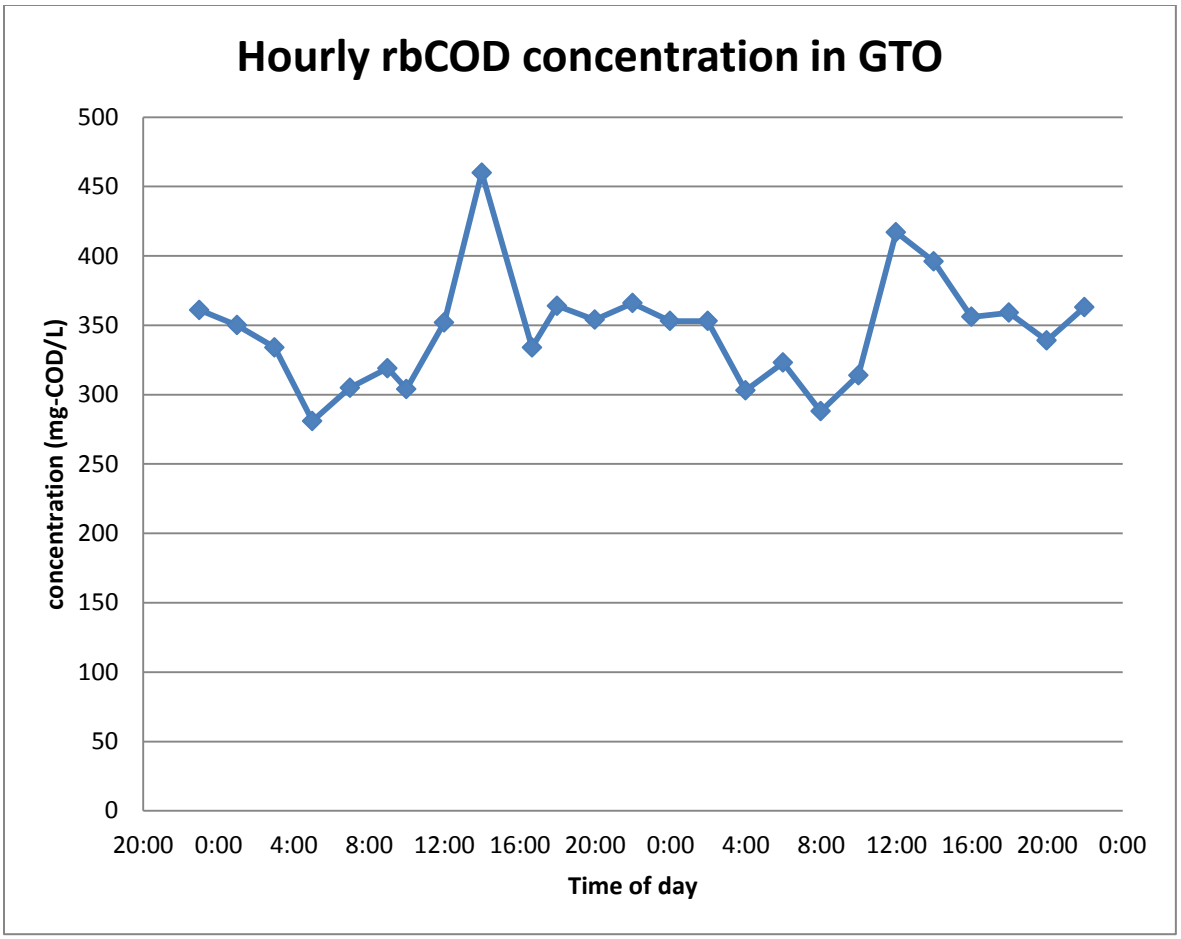

Figure 15. Diurnal pattern of rbCOD in the GTO.

Table 7, below, shows the rbCOD concentration in the GTO for individual gravity thickeners with different operational schemes. The normal operation category describes a gravity thickener that is being operated normally with an average gravity thickener sludge blanket height of 6ft. The increased blanket category describes a gravity thickener that is being operated at a constant sludge blanket height of 8 ft. The elutriated category describes a gravity thickener that is being operated with the elutriation loop implemented; the elutriation rate is between 24 and 48 gallons per minute. The average concentration values reported below were calculated from the entire rbCOD data collected during the study. The same general relative pattern of values between different schemes was consistent in all data sets.

rbCOD concentration (mg-COD/L)		
Normal operation	Increased Blanket	Elutriated
260	411	315

Table 7. Observed average rbCOD concentrations in the GTO under three different gravity thickener operational schemes.

Using a two tailed paired T-test the rbCOD concentration from a gravity thickener with an increased blanket is statistically different from the rbCOD concentration in a gravity thickener with normal operation (p value = 0.003) and the rbCOD concentration from a gravity thickener with an elutriation loop is significantly different that a gravity thickener under normal operation (p value = 0.005). The increased blanket and elutriation are not statistically different from each other (p value > 0.05).

Figure 17, below, shows the VFA concentration in the GTO as a function of sludge blanket height in the gravity thickener. Note that this dataset is composed of grab samples taken around the same approximate time during the daylight hours. The diurnal VFA data is excluded from this data set.

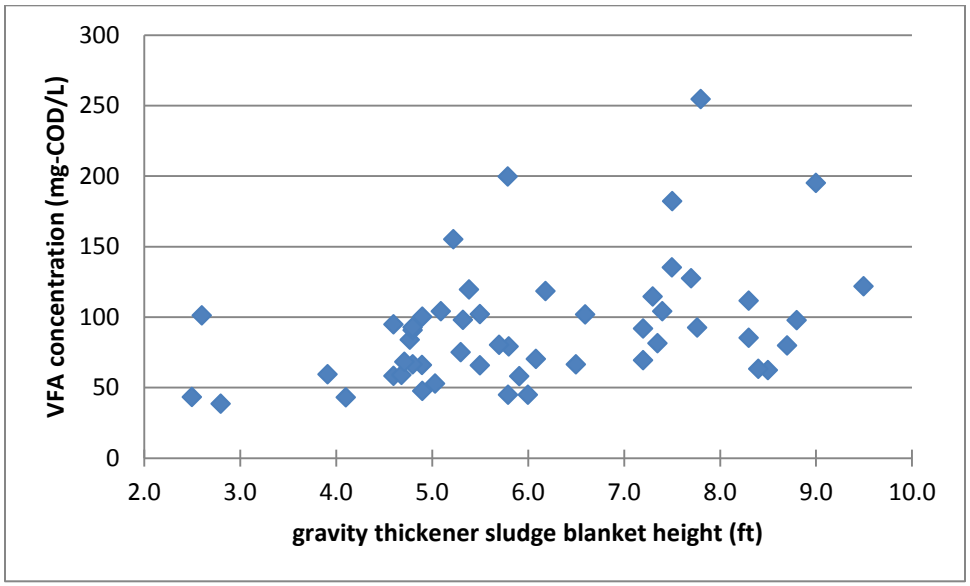

Figure 16. VFA concentration in the GTO verses gravity thickener sludge blanket height at time of sampling.

Table 8, below, shows the average relative speciation of the VFA in the GTO. The average relative percentage of each VFA species was highly consistent throughout every VFA dataset and between all gravity thickeners.

Average Relative Speciation of VFA in GTO (%)				
acetic acid	propionic acid	butyric acid	valeric acid	caprioc acid
50	33.5	13	< 2	< 2

Table 8. Shows the relative speciation of VFA in the GTO

The dominate species of VFA was consistently acetic acid (50%), followed by propionic acid at an average of 33.5%. Butyric acid was the last significant species of VFA present in the GTO and the combination of acetic acid, propionic acid and butyric acid represents over 95% of the total VFA in the GTO.

Table 9, below, shows the ratio of observed carbon loading to the anaerobic RAS reactor in comparison to the observed rate of phosphate removed in the NSEC.

	VFA:P	rbCOD:P	COD:P	BOD:P
phase 1	2.0	3.7	10.3	6.5
phase 2	2.2	3.9	11.1	7.0
phase 3	2.3	4.2	11.9	7.5
phase 4	0	0	0	0
phase 5	2.9	5.2	14.7	9.3
phase 6	3.0	5.5	15.4	9.7

Table 9. Observed carbon to phosphate loading ratio in the NSEC during each study phase.

The observed phosphate removal rate used in the above calculation of the carbon : P ratio was calculated by using a mass balance approach with flow data and daily phosphate composite data sampled from the main influent channel, centrate return to the NSEC, gravity thickener overflow and NSEC effluent. The carbon loading was calculated by using the average daily carbon concentrations in the GTO and flow data from the gravity thickener.

Discussion

The data from the gravity thickener overflow carbon characterization efforts suggests that the concentration of carbon in the GTO is a function of multiple factors. Some of the factors that influence the carbon concentrations in the GTO are time of day, sludge blanket heights in the gravity thickener, and elutriation of gravity thickener sludge from the underflow to the influent splitter box of the gravity thickener.

The observed influence that the time of day plays to carbon concentration in the GTO is likely caused by regular daily fluctuations to influent flows and loading to the plant. Although the relationship between time of day, daily loading patterns and carbon concentration in the GTO is not fully understood, due partially to the complex nature of biological processes and uncontrollable process variations, some useful patterns and trends were discovered. First, carbon concentrations vary hourly in the GTO. Secondly, the variation in the carbon concentrations can happen quickly and be large up to a factor of 3 for VFA. Thirdly, the peak carbon concentrations in the GTO occur approximately around midday and the minimum carbon concentrations occur during the night approximately between midnight and 6am. Fourthly, the daily average carbon concentration is consistent between days in spite of hourly variations.

Generally speaking, the elutriation of gravity thickener underflow to the influent of the gravity thickener increases soluble carbon concentrations in the GTO. Unfortunately, sufficient VFA data was not collected during the elutriation phase of the gravity thickeners to provide comparison to non-elutriated gravity thickener operation. However, sufficient rbCOD data was collected during the elutriation phase which shows that implementation of an elutriation schemes increase the rbCOD concentration in the

GTO. Even though we don't have data to support the claim that elutriation schemes on the gravity thickener increases VFA concentration in the GTO, published literature states that elutriation is a key modification to fermenter and prefermenters operation to increase VFA concentrations in the effluent (Ahn et al., 2006, Bouzas et al., 2007, Chanona at al., 2006). To maximize the soluble carbon (VFA and rbCOD) loading to the anaerobic RAS reactor an elutriation scheme should be implemented on the gravity thickener.

Through the implementation of an elutriation scheme, at a higher rate, it may be possible to increase soluble carbon loading in the GTO to even higher concentrations than observed during the EBPR demonstration. During the EBPR study, the elutriation rate used on the gravity thickener was between 0.5% and 1% of the influent flow to the gravity thickener. The study by Bouzas et al. (2006) showed that a high elutriation rate equal to 12% of the influent flow maximized VFA concentration in the effluent. The results from the previous study suggest that the VFA concentration in the GTO could be further increased if the elutriation rates were increased. At MWRD, the low elutriation rates were used during the full scale study because it was cost effective to use an existing gravity thickener redundant underflow pump as the elutriation pump. In retrospect, the existing gravity thickener redundant underflow pump that was used for the elutriation scheme was undersized and the use of a larger elutriation pump would have allowed better evaluation of the impacts that elutriation has on soluble carbon concentrations in the GTO. Further work using high elutriation rates in the gravity thickener needs to be conducted to fully understand the maximum VFA concentration that can be derived from implementation of an elutriation scheme on the gravity thickener.

Fermentation of COD in the sludge blanket in the gravity thickener is the origin of a significant fraction of the soluble carbon (VFA and rbCOD) that is conveyed to the anaerobic RAS reactors. When the sludge blankets are maintained at high depths, the relative solids concentration in the sludge blankets is higher due to type III (hindered or zone settling) and type IV (compression settling) settling. Multiple studies have concluded that fermentation rates in fermenters and prefermenters are higher at increased solids concentrations and more VFA is produced per unit time (Bouzas et al. 2006, Ahn et al. 2006, Bouzas et al. 2007, Ferrer and Seco 2007, Chanona et al. 2006). The literature is in agreement with the data collected during the gravity thickener overflow carbon characterization. Table 7 and figure 17 shows that both rbCOD and VFA concentrations in the GTO increase with increased sludge blanket depths in the gravity thickener. The increased soluble carbon concentrations in the GTO are a result of both increased solids concentration in the gravity thickener sludge blankets and as a result of the slightly longer SRT of primary solids when the sludge blankets are higher. The slightly longer SRT allows marginally more retention time for solubilization and fermentation reaction to occur in the gravity thickener. To maximize soluble carbon loading to the anaerobic RAS reactor the sludge blankets should be consistently maintained at high sludge blanket depths.

The relative speciation of VFA in the GTO is in agreement with reported literature values of the relative abundance of acetic, propionic, butyric, caprioc and valeric acids present as fermentation end-products of primary solids in municipal wastewaters. See, table 10, below, for a comparison of reported literature values to observed VFA speciation.

Average Relative Speciation of VFA (%)					
	acetic acid	propionic acid	butyric acid	valeric acid	caprioc acid
Observed in GTO	50	33.5	13	< 2	< 2
Literature	38 - 50	36 - 44	9 - 16	5 - 10	N/A

Table 10. Comparison of literature value to values observed in the GTO in regards to the relative speciation of VFA species present in the GTO from fermentation.

The relatively high percentage of VFA as propionic acid in the GTO may limit GAO competition. A study by Thomas et al. (2003), suggests when propionic acid is used as a carbon source for anaerobic VFA uptake, GAO competition is limited. While there is insufficient evidence to support such claims in regards to MWRD's EBPR configuration, it is a possibility. There were no formal PAO / GAO competition evaluations or experiments conducted during this study. In agreement with the literature, it is possible that using a diverse speciation of VFA as a carbon source could be beneficial to the efficiency of this EBPR configuration.

Contradictory to the published literature and US EPA design guidance manual for EBPR processes, NSEC effluent phosphate concentration were extremely low even though the carbon loading from the GTO to the anaerobic RAS reactor was below the reported minimum carbon requirement needed for EBPR process. It may be possible that the EBPR carbon deficit is accounted for by the VFA loading in the main influent channel but this is unlikely because the main influent channel has significant nitrate concentrations and additional phosphate release was not observed in the anoxic compartments of the MLE trains. See table 11, below, for the reported minimum carbon to phosphate ratio in comparison to the observed ratios during the study. All of the observed ratios are less than half of the reported minimums.

Minimum reported carbon to phosphate requirement for EBPR in comparison to observed ratio during the EBPR study		
Substrate measure	**Literature Minimum Substrate : P ratio**	**Average Observed Substrate : P ratio**
$cBOD_5$	20:1	6.5 – 9.7
$sBOD_5$	15:1	
COD	45:1	10.3 – 15.5
VFA	7:1 to 10:1	2.0 – 3.0
rbCOD	15:1	3.7 – 5.5

Table 11. Comparison of observed carbon substrate to phosphate ratio to reported minimum ratio values.

The literature values would suggest that the GTO alone would not be able to sufficiently supply enough carbon to the anaerobic RAS reactor to support EBPR. It is unknown why the EBPR configuration is capable of excellent phosphate removal in spite of carbon limitation in the anaerobic stage, according to conventional design criteria. This represents an area where further work is needed and raises questions that should be investigated. Some of these questions are listed below.

- Is there an attribute of using GTO as a carbon source that reduces the carbon requirement during the anaerobic VFA uptake stage?
    - Is hydrolysis and fermentation of particulate COD happening in the anaerobic RAS reactor and making up the VFA deficit?

- Is the novel side stream EBPR configuration significantly more carbon efficient than mainstream configurations, and if so, why?
    - Does only a conveying a portion (~20%) of the RAS through the anaerobic RAS reactor decrease the VFA requirement compared to a mainstream EBPR configuration?
    - Does the low mixing energy in the anaerobic RAS reactor allows for formation of unusually large floc particulates that contribute VFA by fermentation reactions occurring on the inside of the particles?
    - Does the isolation of the anaerobic RAS reactor from electron acceptor rich recycle streams decrease the VFA requirement?
    - Is there some attribute of using the high RAS concentrations in the anaerobic RAS reactor that allows the process to be more efficient?

CHAPTER VI

Phosphate profiling

Introduction

To gain a more in-depth understanding of the novel EBPR configuration and to help trouble shoot EBPR performance upsets during the study; extensive phosphate profiling was conducted on the anaerobic RAS reactor, MLE aeration basins, secondary clarifier overflow and final NSEC effluent. The phosphate profiling was conducted in a consistent manner at predetermined locations to allow comparison of profiles from different time and under different operating conditions.

Online phosphate meters are either very expensive and/or do not work reliably, as was the case at MWRD during the EBPR demonstration. It was very important to collect good dataset to use as evidence to justify operational changes during the study and this necessitated a continual need to manually collect phosphate profiles throughout the plant. The phosphate profiling effort allowed MWRD staff a way to examine important EBPR process conditions throughout the study. The phosphate profiling was useful in, but not limited to, examining secondary phosphate release in the blankets of the final clarifiers, aerobic phosphate mass uptake and examining different sources of phosphate loading to the NSEC.

Also using a mass balance approach around the anaerobic RAS reactor, the phosphate profiling data collected was fundamental to the development of anaerobic phosphate release rates (APRR) observed in the anaerobic RAS reactor during the study. The APRR was calculated as the change in phosphate mass between the influent of the anaerobic RAS reactor and the effluent of the anaerobic RAS reactor. According to the

literature, the downstream aerobic phosphate uptake capacity is directly proportional to the anaerobic phosphate release (Comeau et al. 1987). The APRR is easily measured and was used as a surrogate measure to help diagnosed EBPR system upsets. See equation 1, below, for the definition of the APRR calculation.

$$APRR = C_{ARR}Q_{ARR} - (C_{GTO}Q_{GTO} + C_{RAS}Q_{RAS}) \quad (1)$$

Where,

C_{ARR} = phosphate concentration in anaerobic RAS reactor effluent

Q_{ARR} = total anaerobic RAS reactor flow

C_{GTO} = phosphate concentration of the GTO

Q_{GTO} = GTO flow to the anaerobic RAS reactor

C_{RAS} = phosphate concentration of the RAS

Q_{RAS} = RAS flow to the anaerobic RAS reactor

When the APRR is coupled with the influent phosphate loading to the aeration basin (APRR fraction) a relationship between the phosphate loading and phosphate removal capacity is developed. The dimensionless parameter that describes this coupling of the phosphate removal capacity and the phosphate loading is defined as the APRR fraction. See equation 2, below, for the definition of APRR fraction.

$$\text{APRR fraction} = \frac{APRR}{TPL} \quad (2)$$

Where,

APRR = anaerobic phosphate release rate

TPL = total phosphate loading rate to aeration basins

To understand the EBPR process and identify potential areas for process optimization it is important to quantify all phosphate loading to the aeration basins where the aerobic phosphate uptake occurs. The origin of phosphate loading to the influent of

the MLE aeration basins comes from influent flows, return flows and recycle flows. An influent phosphate load is defined as a phosphate originating from outside the plant in the influent flows. A return phosphate load is defined as phosphate was once removed or sequestered from the liquid phase and then was released back to the liquid phase. A recycle phosphate load is defined as phosphate that is internally recycled within the plant that is not removed from the liquid phase. The influent flows that contribute phosphate to the influent of the MLE aeration basins are the main channel influent to the NSEC and influent phosphate in the GTO being conveyed to the anaerobic RAS reactor. The recycle flows that contribute phosphate to the influent of the MLE aeration basins are the mixed liquor return (MLR) and RAS flow. The return flows that contributes to phosphate loading in the influent of the NSEC MLE trains are the centrate return flow from dewatering of solids in centrifuges after anaerobic digestion and the anaerobic phosphate release that occurs in the anaerobic RAS reactor. A central use of the phosphate profiling in the NSEC was that it allowed MWRD staff a way to compare EBPR process performance under different phosphate loading scenarios. Additionally, the phosphate profiling coupled with a mass balance approach helped elucidated important phosphate feedback loops that were initially overlooked.

The phosphate profiling in the anaerobic RAS reactor also allowed the MWRD staff a tool to investigate if the volume and small footprint of the anaerobic RAS reactor was sufficiently sized. Since the anaerobic RAS reactor is a side stream configuration, the conventional EBPR design criteria may not be directly applicable and the phosphate profiling allowed an avenue to evaluate if the retention time in the anaerobic RAS reactor is appropriate for proper anaerobic VFA uptake. Using the phosphate profiling data, we

were able to use the anaerobic RAS reactor phosphate profiling to postulate the minimum size requirement of this EBPR configuration.

Methodology

Anaerobic Reactor Profiling

Five permanent anchored sample lines were installed in the anaerobic RAS reactor to enable consistent sample collection locations along the length of the anaerobic RAS reactor and at different depths. The permanent anchored sampling lines allowed us to better study the solid stratifications in the anaerobic reactor and phosphate release profile. The anchored sample lines consisted of a 16lb rubber coated mushroom anchor attached to a 17ft coated steel cable. The anchored lines had two 3/8 inch nylon tubes attached to them. One tube went to the bottom of the anchored sample line (14 feet depth below water surface), while the second tube went to the middle of the anchored sample line (7 feet below water surface). When the anchored sample lines are submerged one tube would be at the bottom of the anaerobic RAS reactor and the other would be in the middle of the water column. An auto-sampler pumping head was used to collect grab samples from the anchored sample lines, the auto-sampler would first purge the sample lines with air, then pump 3L of sample. The 100mL aliquots of sample used for analysis were only taken after the sample lines had 3L of fresh sample pumped through the tubing. The consistent sample collection procedure of initial sample line purging and 3L pumping of fresh sample allows for representative data.

Six 100mL samples were taken along the length of the anaerobic reactor from approximately 9% to 100% of the HRT of the anaerobic reactor, the samples in the anaerobic RAS reactor were collected at the middle depth of the anaerobic reactor (7ft).

100mL grab samples of the GTO and RAS were also collected. The RAS sample was collected from the South Waste Activated Sludge sampling location in the south NSEC gallery. The GTO sample was collected from the gravity thickener overflow weir.

Time of sampling was recorded for every sample taken. For anaerobic RAS reactor phosphate profiling, the initial phosphate concentration was calculated as the theoretical concentration based off the known GTO and RAS flows and phosphate concentration of the RAS and GTO.

When phosphate samples were collected, they were immediately filtered through a 0.45um glass fiber filter using a hand vacuum pump and a flip-mate filter apparatus. The phosphate analysis was done using a HACH DR 3900 spectrophotometer using either a low range powder pillow method or a high range molybolium ampules method. Duplicate and verification samples were submitted to Technical Services Laboratory to verify the accuracy of the HACH spectrophotometer method. The TSS analysis was conducted by the Technical Services Laboratory following standard laboratory procedure.

Aeration Basin Profiling

Surface grab samples were collected from the aeration basin at six predetermined and equally spaced locations. A grab sample was collected in the main influent channel downstream of main influent channel mixers. The first aeration basin sample is located at the end of the anoxic zone, directly upstream of the first aerated zone. The following five sample locations are equally spaced to the end of the aerated tank. The influent loading is calculated using the influent flow and the main channel concentrations plus the MLR flow and the aeration basin effluent phosphate concentrations. This approach compensates the data for dilution effects of mixing the MLR and main channel influent.

Secondary Clarifier and final NSEC effluent Profiling

Surface grab samples were taken from the final clarifier overflow weirs, the time of sampling was recorded. Grab samples of the NSEC final effluent were taken from the north nitrification sampling location. A permanent composite auto-sampler was used to draw 100mL aliquots of sample from the NSEC final effluent channel directly upstream of the disinfection process. This sample location has an average flow of approximately 95 MGD and originates from the combination of flows from all twelve final secondary clarifier overflows in the NSEC.

Online and Composite sampling in the NSEC

Online TSS and pH instrumentation exist in the anaerobic RAS reactor, CaRRB and MLE aeration basins. Permanent daily composite auto-samplers were in operation on the NSEC final effluent, NSEC main influent channel, GTO and CaRRB reactors during the duration of the study. The daily composite samples were analyzed for phosphate and total phosphorus by the Technical Services Laboratory four times per week.

Additionally a ChemScan online monitor was installed on the anaerobic RAS reactor effluent, CaRRB effluent and NSEC main influent channel. The ChemScan continuously monitored phosphate, nitrate and nitrite concentrations.

Results

Observed Secondary Phosphate Release

The difference between the final clarifier effluent phosphate concentration and the effluent phosphate concentration from the MLE aeration basins is the observed secondary phosphate release that occurs in the sludge blankets of the final clarifiers. The MLE

aeration basin effluent phosphate and final clarifier effluent phosphate concentrations were sampled at the same time and from the same MLE/final clarifier sequence. Table 12, below, summarizes the observed secondary release in the final clarifiers, note this data is composed from coupled grab samples.

Observed Secondary Phosphate Release Occurring in the Final Clarifier (mg-P/L)												
MLE PO_4 effluent	0.02	0.03	0.03	0.10	0.48	0.54	0.70	1.00	1.40	1.74	2.20	3.70
Final Clarifier PO_4 effluent	0.04	0.20	0.12	0.11	0.09	0.82	0.57	1.22	1.36	1.83	2.20	3.70
Difference	+ 0.02	+ 0.17	+ 0.09	+ 0.01	- 0.39	+ 0.28	- 0.13	+ 0.22	- 0.04	+ 0.09	0	0

Table 12. Summary of observed secondary phosphate release that occurs in the final clarifier.

The secondary phosphate release in the final clarifiers in the NSEC is minimal, the largest observed secondary release was 0.28 mg-P/L, while the average observed secondary release was 0.09 mg-P/L. Using a 2 tailed paired T-test, the phosphate concentration in the aeration basin effluent is not statistically different than the final NSEC effluent phosphate concentration (p value > 0.05). On three separate sampling events there was an additional observed phosphate uptake occurring in the final clarifiers.

Aeration Basin Phosphate Loading flows

The average total daily phosphate loading to the NSEC MLE aeration basins is approximately 6000 kg-P/d. Table 13, below, a summary of the average, minimum, maximum, range and percentage of total phosphate loading observed in the NSEC from the influent, recycle and return flows to the MLE aeration basins.

	Influent Loading (kg-P/d)		Recycle Loading (kg-P/d)		Return Loading (kg-P/d)	
	Main Channel	**GTO**	**MLR**	**RAS**	**Centrate**	**APRR**
Average	1633	166	1450	630	642	1490
Maximum	2100	291	6410	1330	950	2110
Minimum	1300	108	32	40	270	470
% of total PO_4 load to MLE	27%	3%	24%	10%	11%	25%
Range	800	183	6378	1290	680	1640

Table 13. Summarization of all observed phosphate loading to NSEC MLE aeration basins.

The phosphate loading from influent streams (main channel and GTO) only average about 30% of the total phosphate mass entering the aeration basins. The phosphate recycle loading from MLR and RAS flows compose an average of 34% of the phosphate mass entering the aeration basins. The largest source of phosphate loading to the aeration basin comes from return loading in the centrate flow from anaerobic digestion and APRR from the anaerobic RAS reactor. The return flows account for an average of 36% of the phosphate mass entering the aeration basins. It is important to mention that the recycle loading from the MLR and RAS flows show the largest degree of variation between the observed minimum and maximum phosphate loading to the aeration basins. The influent phosphate loading from the main channel and the GTO show the smallest amount of variation between minimum and maximum phosphate loading to the aeration basin. The return loading from APRR and centrate return flows

show a moderate range of variation between minimum and maximum phosphate loading to the aeration basins.

There is a definitive correlation between high aeration basin phosphate effluent concentration and an increased phosphate loading from recycle flows. The MLR and RAS flows recycle phosphate from the effluent of the aeration basins back to the influent of the aeration basins; a large portion of the phosphate not removed during the aerobic stage is recycled to the influent. See figure 18 and 19, below, for a plot of observed aeration basin effluent phosphate concentration to MLR and RAS phosphate loading to aeration basin.

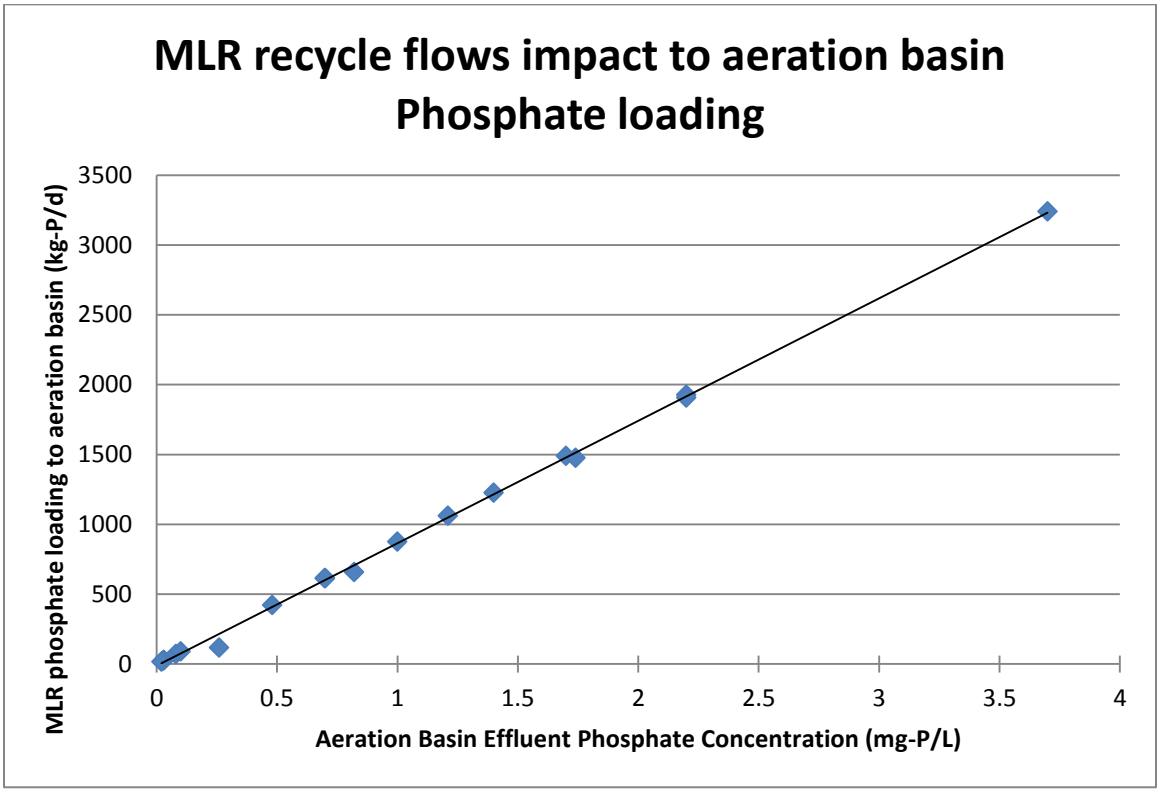

Figure 17. Plot showing the impact that aeration basin effluent phosphate concentration in relation to MLR recycle phosphate loading.

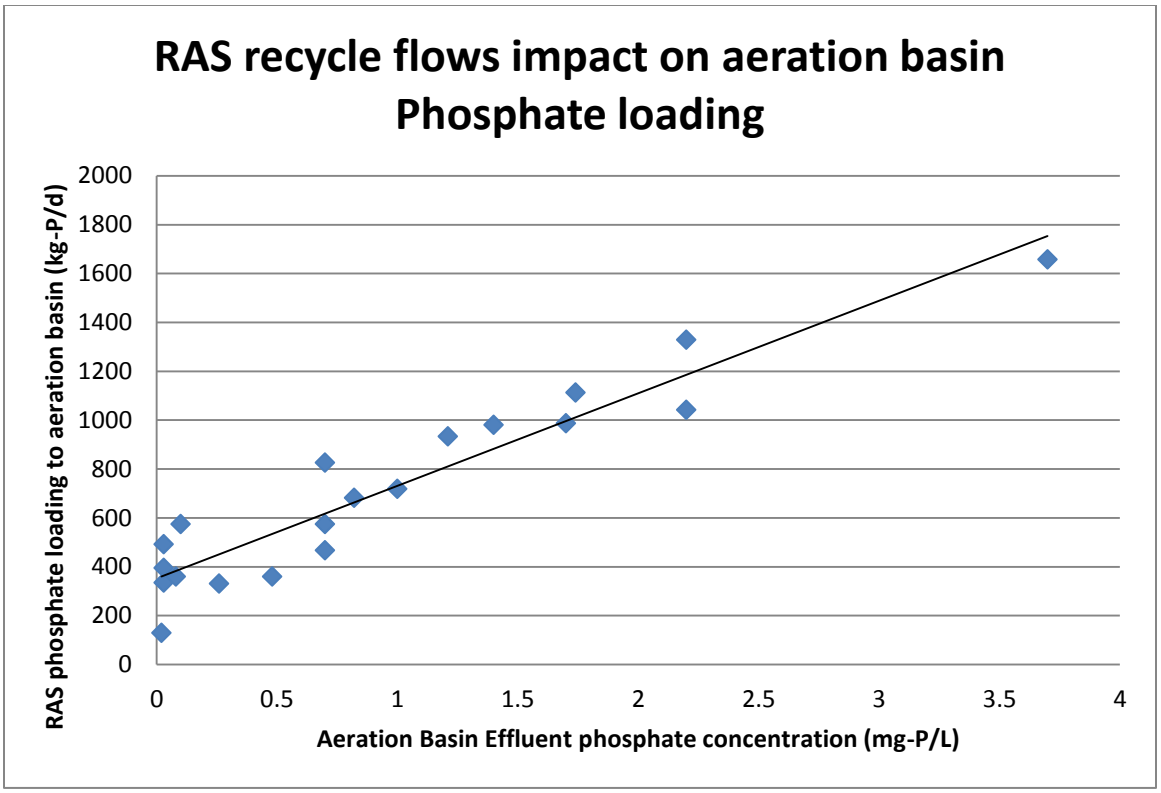

Figure 18. Plot showing the impact that aeration basin effluent phosphate concentration in relation to RAS recycle phosphate loading.

Anaerobic RAS reactor HRT

The phosphate profiling in the anaerobic RAS reactor has a consistent characteristic shape in almost every profile collected. The characteristic shape is composed of two slope trends; the initial slope trend shows rapid phosphate release at the beginning of the reactor which decreases in an asymptotic behavior. This first trend occurs in the first 40% of the HRT of the anaerobic RAS reactor and past this point the second slope trend dominates. The second slope trend is a linear slope than gradually increases until the end of the anaerobic RAS reactor. It is important to note that the first slope trend accounts for greater than 90% of the anaerobic phosphate release, while the

second slope trend is quite flat. See figure 20, below, for a typical phosphate release profile for the anaerobic RAS reactor.

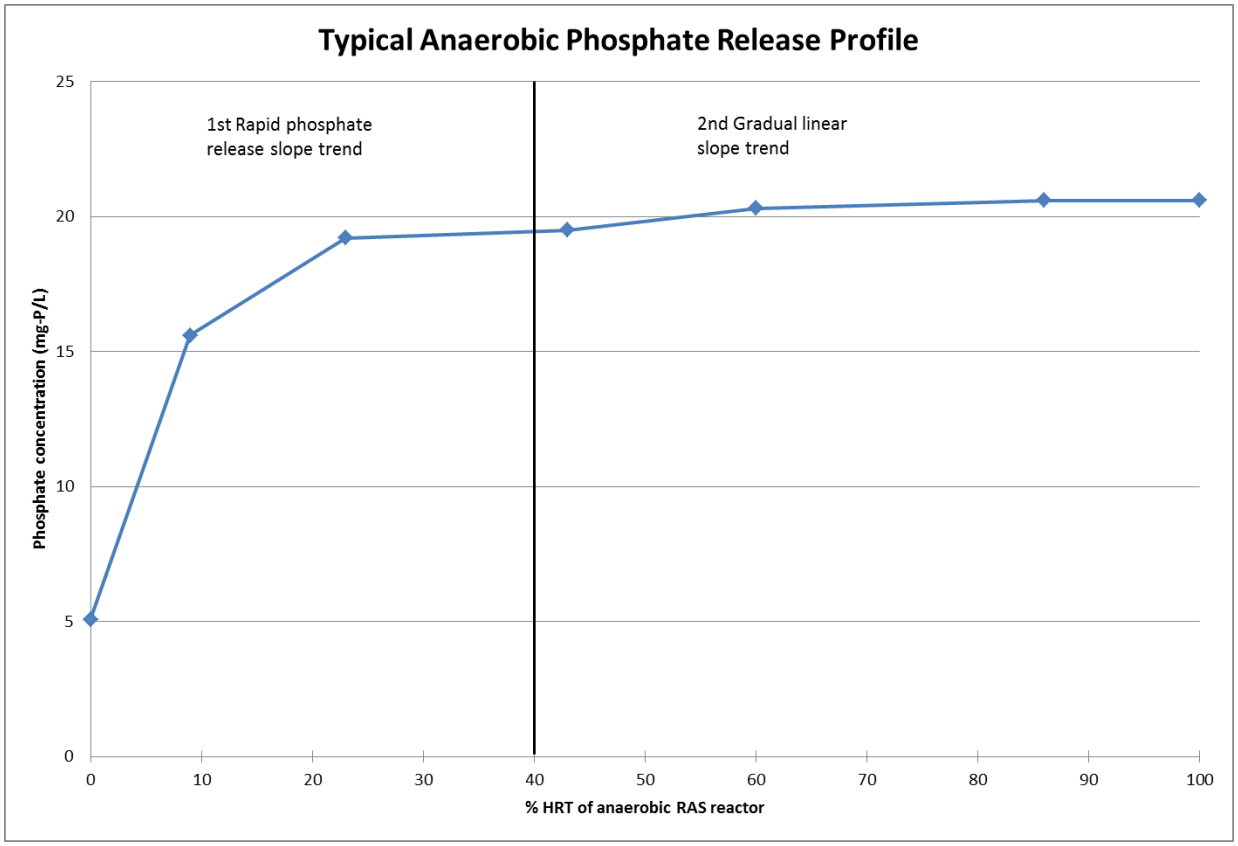

Figure 19. Typical shape of anaerobic RAS reactor phosphate profile.

It is important to note that regardless of influent or effluent anaerobic RAS reactor phosphate concentration, that all anaerobic phosphate release profiles had this same shape, with the exception of profiles collected during the RAS fermentation phase of the study. See figure 21, below, for a plot of three observed anaerobic phosphate release profiles that have the different influent and effluent phosphate concentrations but the same characteristic shape.

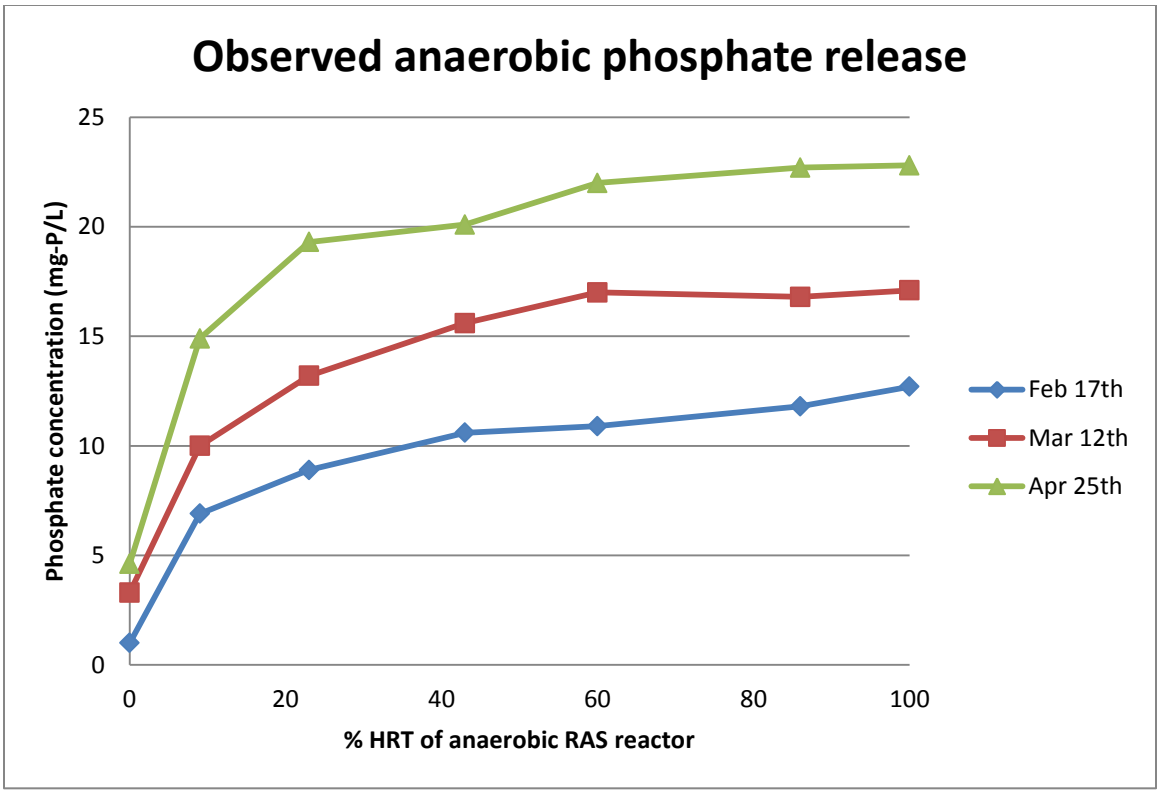

Figure 20. Three typical anaerobic phosphate release profiles showing that the anaerobic phosphate release have the same general shape regardless of influent or effluent phosphate concentrations.

Under normal operation, the HRT of the anaerobic RAS reactor was 65 - 78 minutes depending on the RAS and GTO flows to the anaerobic RAS reactor. The HRT of one pass through the MLE basins was 150 – 210 minutes, depending on number of basins in service and main channel flows. The anoxic compartment at the head of each MLE train composed 1/6 of the total MLE volume, therefore the aerobic retention time of one MLE train was 125 - 178 minutes and the anoxic retention time was 25 - 36 minutes. The range of observed ratios of aerobic retention time to anaerobic time is shown below in table 14.

Observed Ratio of Aerobic Retention Time to Anaerobic Retention Time (min/min)		
Minimum	Average	Maximum
1.60	1.95	2.75

Table 14. Observed ratio of aerobic retention time to anaerobic retention time under normal operation during the EBPR study.

Anoxic Phosphate trend in aeration basin

The phosphate profiling in the MLE aeration basins showed no definitive or significant phosphate release or uptake in the anoxic compartment. The phosphate concentrations remained very constant between the start of the anoxic compartment and the end of the anoxic compartment.

APRR – Anaerobic Phosphate Release Rate

The measured APRR showed a strong correlation to observed aerobic phosphate uptake in the aeration basins. See figure, 22, below for a scatterplot and trend line of the APRR to the observed aerobic phosphate uptake. This figure is composed of all data for the anaerobic phosphate release profile and aerobic phosphate uptake profile pairs collected over the course of the study.

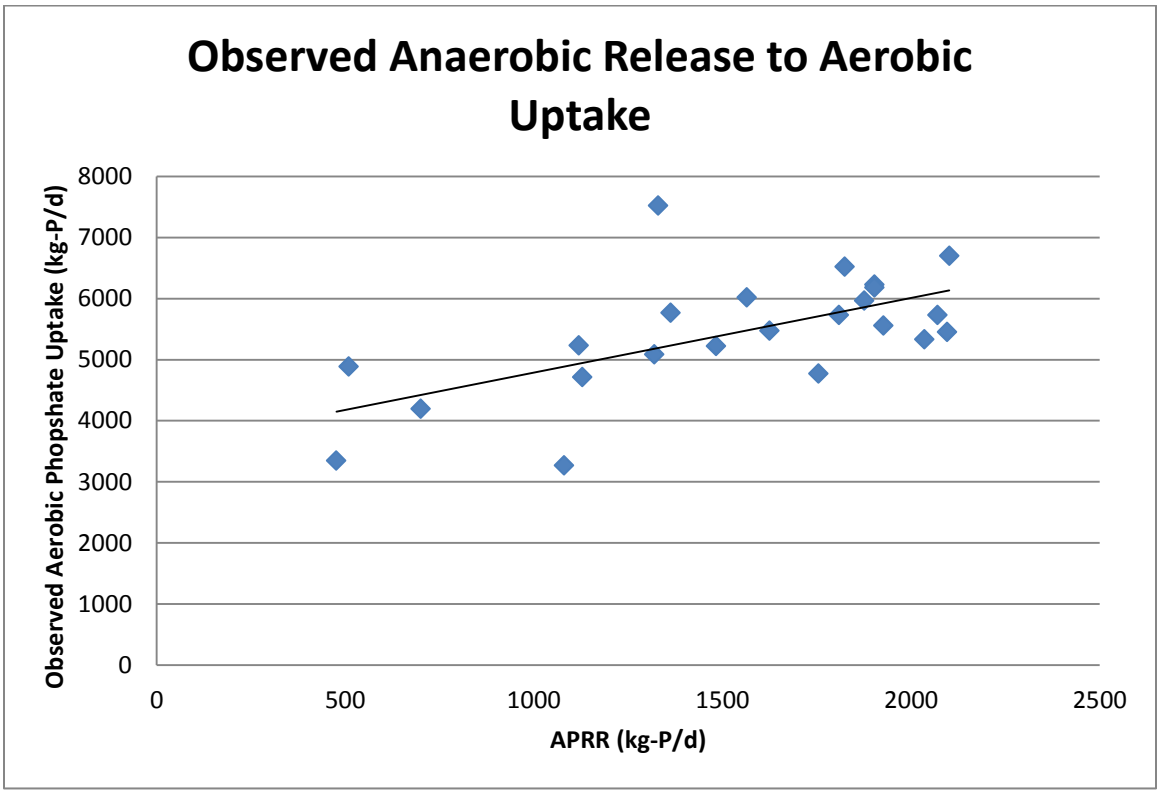

Figure 21. Plot of measured APRR in comparison to observed aerobic phosphate uptake in the the MLE aeartion basins

Figure 20 shows a correlation between the APRR and downstream aerobic phosphate uptake capacity.

The fraction of the total aeration basin phosphate load originating from the APRR (APRR fraction) shows a correlation to the aeration basin effluent phosphate concentration. When the APRR fraction composes 30% or more of the phosphate load to the aeration basin, the aeration basin effluent phosphate concentration is extremely low (< 0.15 mg-P/L). As the APRR fraction decreases below 30%, the aeration basin effluent phosphate concentration increases. See figure 23, below, for a plot of the APRR fraction to the aeration basin effluent phosphate concentration. This figured is composed of all the observed phosphate release and uptake datasets.

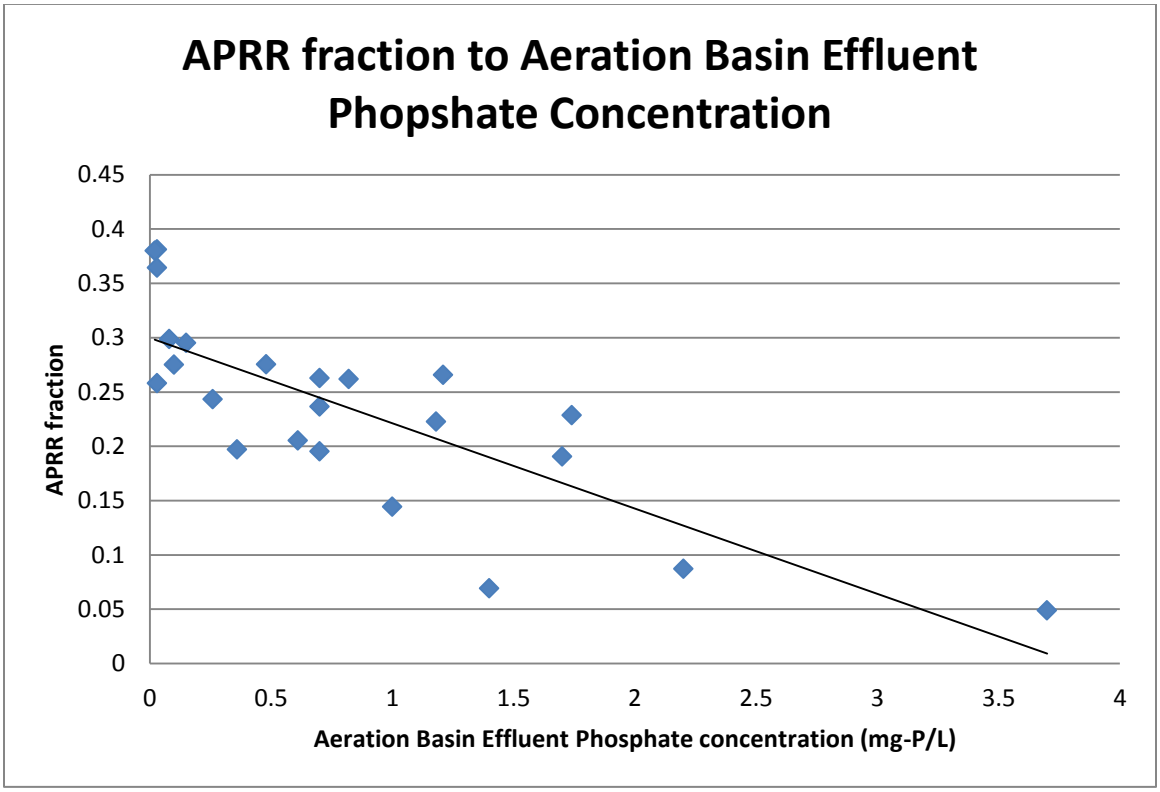

Figure 22. Plot of APRR fraction in comparison to the effluent aeration basin phosphate concentration.

The data in figure 21 suggests that low aeration basin effluent phosphate concentration is a function of APRR fraction.

Anaerobic Solids Retention Time

The anaerobic SRT varied over the EBPR study from a minimum value of 0.25 days to a maximum value of 0.82 days. The data from the study suggests that there is not a strong correlation between the anaerobic SRT and EBPR process performance. Anaerobic SRT did not show a correlation to aerobic phosphate uptake. See figure 24, below, for a plot of anaerobic SRT in comparison to observed aerobic phosphate uptake. This figure is composed of all aerobic phosphate uptake profiles collected with the associated anaerobic SRT on the date of sampling.

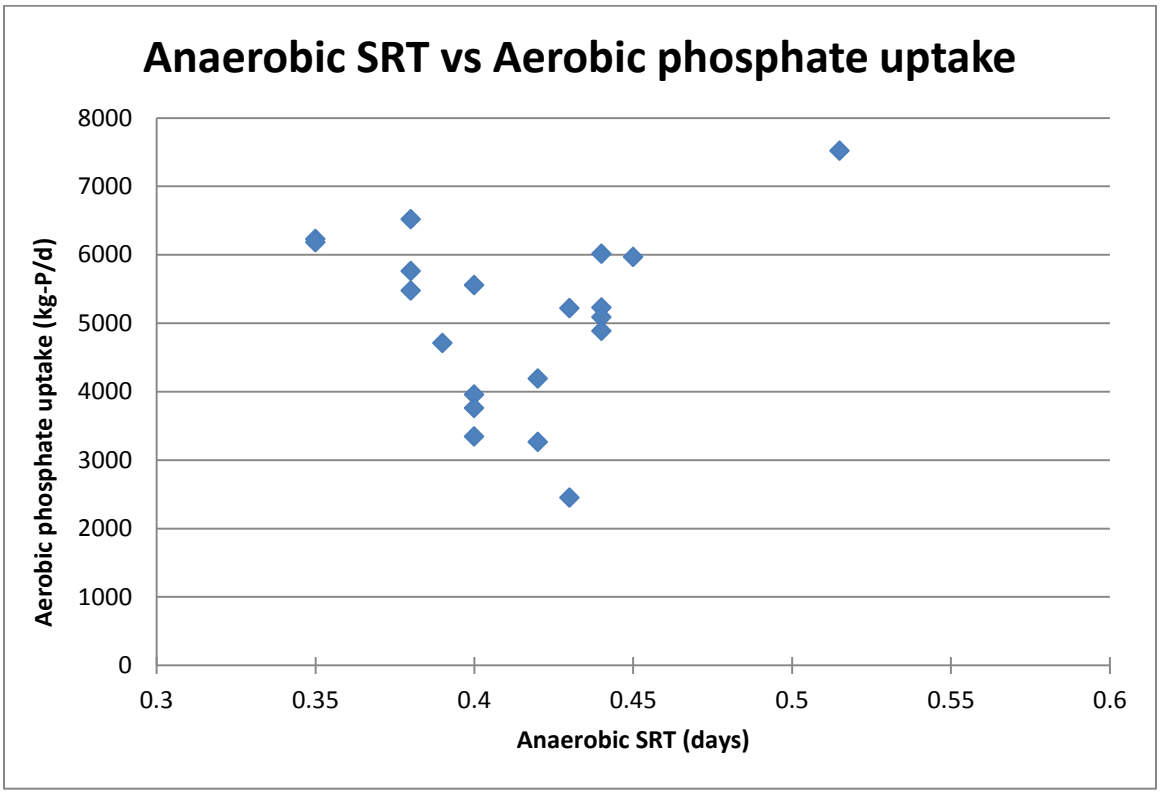

Figure 23. Comparison of anaerobic SRT to aerobic phosphate uptake, this figures no apparent correlation between anaerobic SRT and aerobic uptake rate.

Additionally, anaerobic SRT does not show an apparent correlation to observed MLE aeration basin effluent phosphate concentrations. See figure 25, below, for a plot of anaerobic SRT and MLE aeration basin effluent phosphate concentration.

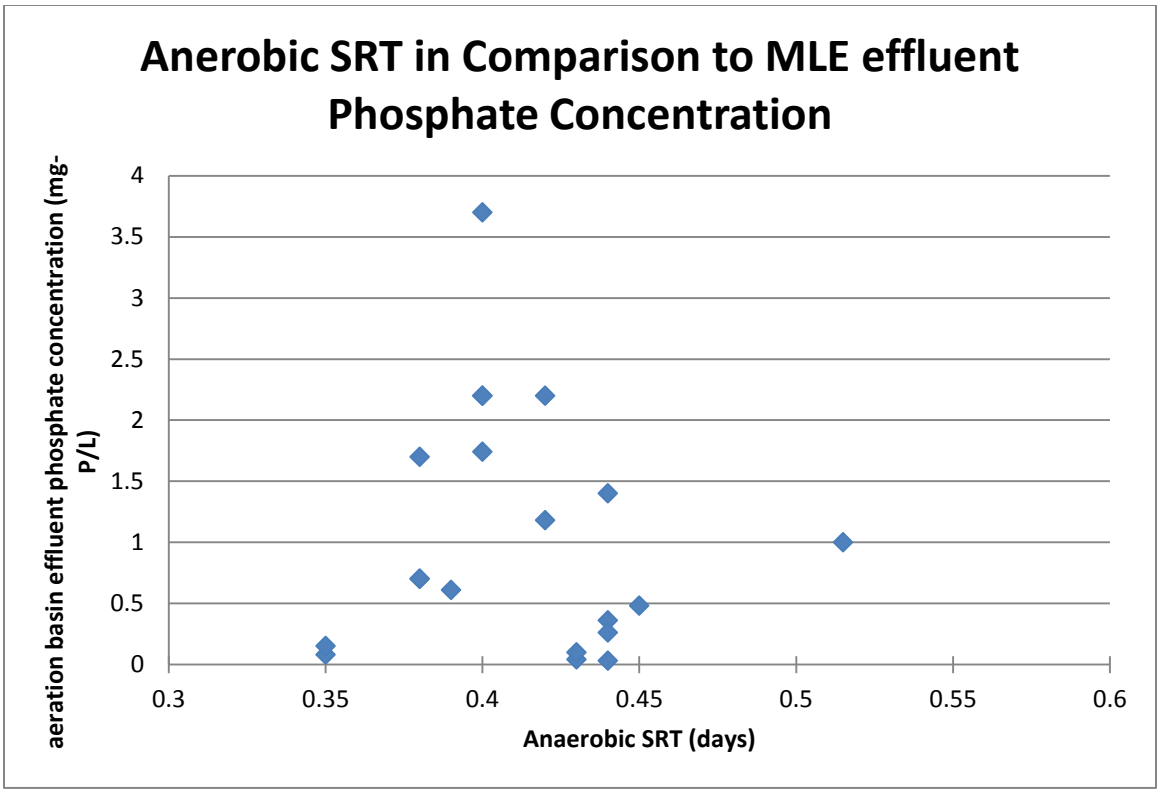

Figure 24. A plot of anaerobic SRT in comparison to aeration basin effluent phosphate concentration, note hat there seems to be no apparent correlation between the two.

Observed Aerobic Phosphate uptake rate

The aerobic phosphate uptake rate ranged between a minimum value of 2450 kg-P/d to a maximum value of 7518 kg-P/d. The average aerobic phosphate uptake rate was 5200 kg-P/d. Figure 26, below, shows a comparison between the observed phosphate uptake rate and the MLE aeration basin effluent phosphate concentration.

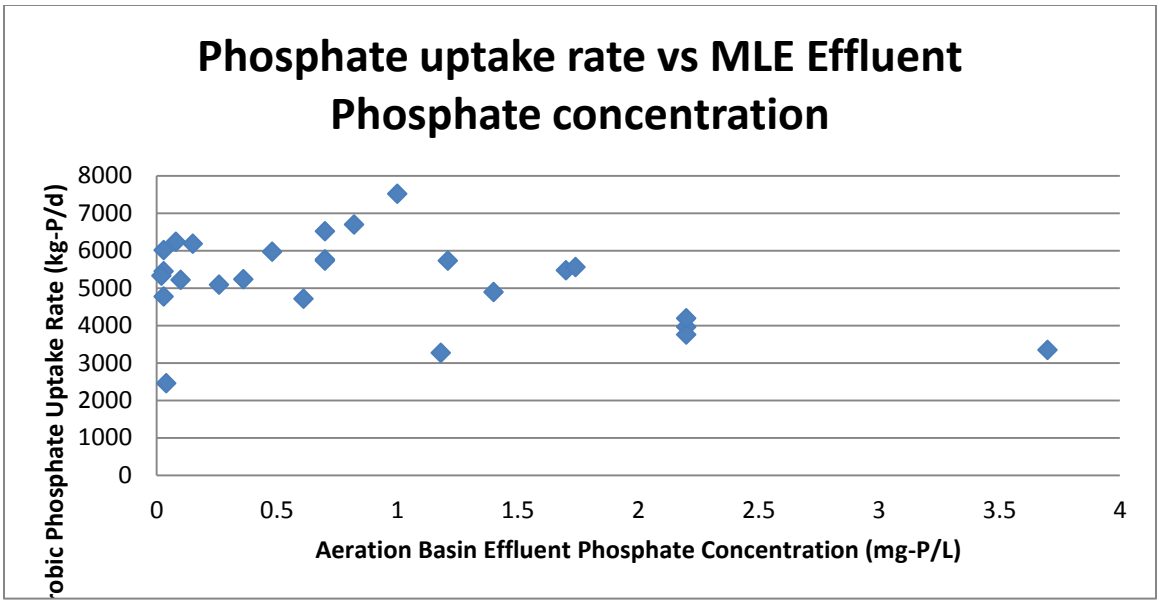

Figure 25. Plot of aerobic phosphate uptake rate in comparison to the effluent phosphate concentration from the aeration basins.

It is important to note that high phosphate uptake rates do not correspond to extremely low MLE aeration basin effluent phosphate concentrations. From the data is appears that when the aerobic phosphate uptake rate exceeds 6000 kg-P/d, then the aeration basin effluent phosphate concentration is always below 1.0 mg-P/L. The high phosphate release rates equate with high phosphate uptake rates even when the effluent phosphate concentration is high because of excess phosphate loading to the MLE aeration basins.

Discussion

Secondary release

Generally speaking, the secondary release and additional phosphate uptake observed in the final clarifiers are insignificant in comparison to the phosphate mass released and/or uptaken in upstream EBPR processes. In comparison to MLE aeration basin total phosphate loading, the maximum observed secondary release (0.28 mg-P/L) observed would be less than 1% of the average phosphate loading to the aeration basins

and the average observed secondary release (0.09 mg-P/L) corresponds to a phosphate load that is equal to less than 0.5% of the average phosphate loading to the aeration basins. The RAS flow rates from the final clarifiers are sufficient to minimize secondary phosphate release in the blankets of the final clarifiers and secondary phosphate release in the final clarifiers does not appear to significantly increase the phosphate concentration in the final NSEC effluent. Future optimization efforts focused on lowering NSEC final effluent phosphate concentrations may be better utilized by examining other process considerations other than secondary phosphate release in the final clarifiers.

Anoxic phosphate trends

Neither anoxic phosphate uptake nor additional anoxic phosphate release happens in the anoxic compartment of the MLE aeration basins. The initial phosphate concentrations at the start of the MLE trains were calculated from the MLR and main channel influent phosphate concentration and flows. This approach compensates for dilution effects and is a more accurate measure of phosphate concentration at the start of the anoxic compartment because a representative sample is difficult to obtain due to mixing of main channel influent and MLR at the head of the compartment.

The operation of the anoxic compartment in the MLE aeration basins should focus on nitrogen removal. The operation of the anoxic zone does not show any apparent beneficial or adverse impacts on EBPR processes, therefore the operation of the anoxic compartment should be based on nitrogen removal considerations and not phosphate removal.

Phosphate loading

The phosphate loading to the MLE aeration basins which requires sequestration during the aerobic phosphate uptake phase is far in excess of the influent phosphate loads to the NSEC primarily due to recycle and return flows. The recycle and return phosphate flows are not good for efficient phosphate removal, because not only do they increase the phosphate mass to the aeration basin but they also can fluctuate which produces phosphate surges that can cause unstable effluent phosphate concentrations. For stable EBPR performance and consistently low effluent phosphate concentrations there need to a correct balance between phosphate loading and EBPR phosphate uptake capacity.

MLR and RAS recycle phosphate flows are directly related to the aeration basin effluent phosphate concentrations and can be reduced by operational control strategies. When MLR flow rates are reduced the MLR phosphate recycle loop is proportionally decreased. Likewise, when the RAS flow rates are decreased the RAS phosphate recycle loop is decreased. It is of interest to minimize the recycle phosphate loading to the aeration basins but there are practical limits to the amount that the MLR and RAS flow rates can be decreased. In addition to practical limits that the recycle flows can be reduced, it is important to meet all other treatment objectives and the reducing the recycle flows can impacts other treatment processes, such as de-nitrification. The other factor that influences the phosphate recycle loading is the concentration of phosphate in the aeration basin effluent. Stable low phosphate concentrations in the aeration basin effluent will minimize the adverse impacts of phosphate recycle loading independent of recycle flow rates. Consistently maintaining low effluent phosphate concentrations is the best way to minimize the phosphate recycle loading because the MLR and RAS flow rates can be altered to meet other treatment objectives.

The return phosphate loading from the centrate and APRR are significant. Unlike other phosphate loading flows to the aeration basins the APRR is beneficial to aerobic phosphate uptake, and because of this, the operation of the EBPR configuration should strive to maximize the APRR. Increasing the ferric chloride dose to the centrate return flow will result in reduced phosphate loading from the centrate return stream. The ferric chloride will precipitate a portion of the phosphate in the centrate return and this will effectively reduce the phosphate loading to the aeration basins. Chemical precipitation of phosphate is commonly used at other WWTP with EBPR configurations to treat centrate return flows. Since centrate return composes a significant portion of the phosphate loading to the aeration basins there is a large potential advantage to precipitating the phosphate in the centrate before it gets back to the aerations basins. This approach is both easy to implement in the NSEC and would be very beneficial to assist in producing low effluent phosphate concentrations.

The novel EBPR configuration is capable of removing the influent phosphate load from the main channel influent and the GTO. When the recycle and return phosphate loads are stabilized, the system is capable of producing low very effluent phosphate concentrations. APRR is beneficial and should be maximized; centrate return phosphate loading can be easily reduced by increasing ferric chloride feeds to the centrate flow after dewatering. The recycle phosphate loading in the MLR and RAS becomes insignificant when the aeration basin effluent phosphate concentrations are maintained at low levels. Therefore, the best practice to stabilize and reduce the phosphate loading to the aeration basins would be to use ferric chloride (or another metal-salt) to precipitate the phosphate in the centrate return. If this reduces the phosphate loading below the phosphate uptake

capacity then, the recycle phosphate loading in the MLR and RAS becomes insignificant, when aeration basin effluent phosphate concentrations are low.

Footprint of anaerobic RAS reactor

The anaerobic RAS reactor phosphate profiling data shows that the hydraulic retention time of the anaerobic RAS reactor is sufficiently long enough to allow for anaerobic VFA uptake to occur. The ratio of aerobic HRT to anaerobic HRT is approximately 2. In comparison to the reported literature values where optimal phosphate removal was observed at an aerobic HRT to anaerobic HRT ratio between 3 and 4 (Neethling et al., 2005), the anaerobic HRT should be sufficiently sized to allow for sufficient anaerobic VFA uptake.

The shape anaerobic phosphate release profiles are consistent in all of the anaerobic RAS reactor phosphate profiles. If you assume that the anaerobic VFA uptake follows a basic Michaelis-Menten kinetic enzyme model, where VFA is the substrate and phosphate is the product of the anaerobic VFA uptake reaction, then the shape of the anaerobic phosphate release curve is identical to predicted product accumulation (phosphate release). See figure 27, below, for an arbitrary example of the predicted shape of Michaelis-Menten kinetic model.

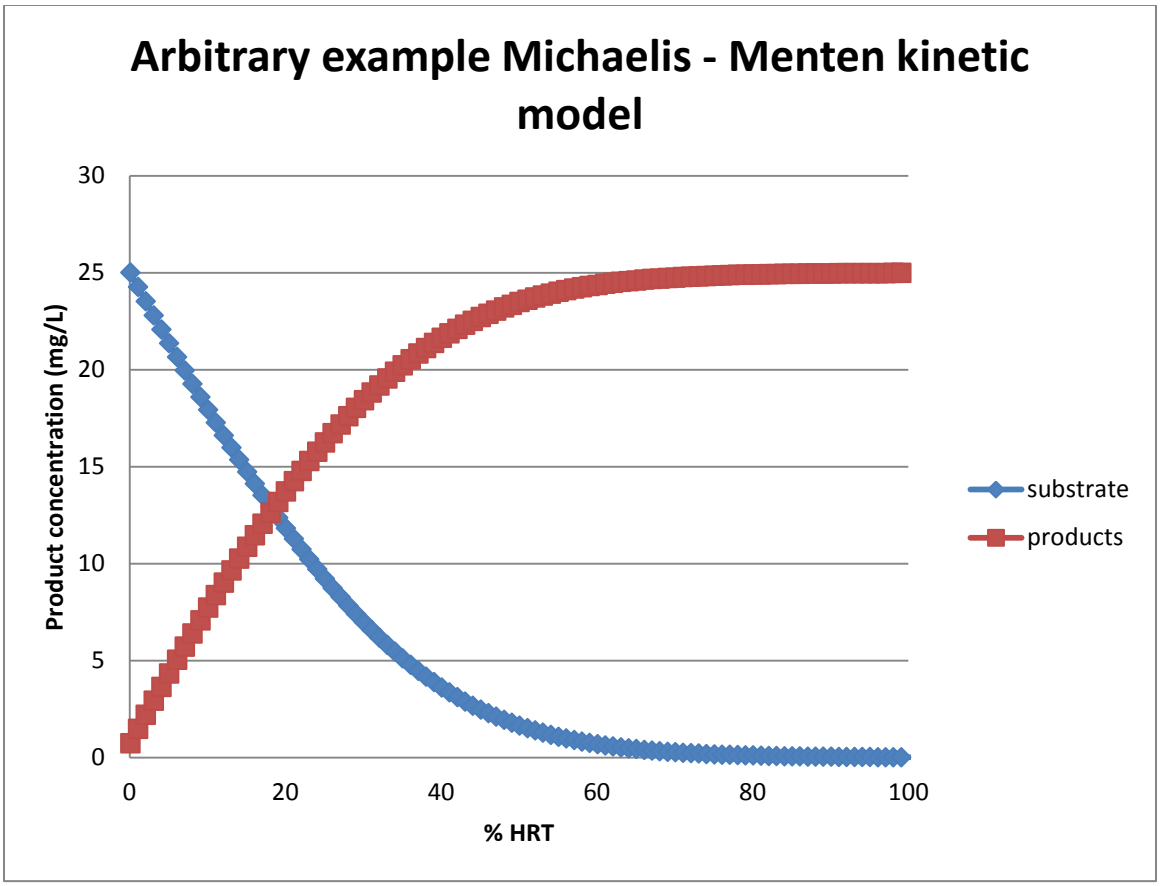

Figure 26. Arbitrary example of Michalis-Menten kinetic model where.

The Michaelis-Menten kinetic model is the simplest and best known model of enzyme kinetics and it is not impossible to assume that anaerobic VFA uptake could exhibit a similar behavior. The Michaelis-Menten enzyme kinetic model is defined below.

$$\frac{dS}{dt} = \frac{-V_{max}S}{K_m+S} \quad (3)$$

$$\frac{dP}{dt} = \frac{V_{max}S}{K_m+S} \quad (4)$$

Where,
dS/dt = the rate of change of substrate
dP/dt = the rate of change of products
V_{max} = maximum specific substrate degradation coefficient
K_m = the half saturation concentration of the substrate
S = substrate concentration

The point is that the quick initial release and then gradual asymptotic behavior observed in the anaerobic phosphate release profiles in the anaerobic RAS reactor is very similar to the predicted behavior of products in the Michaelis-Menten kinetic model. The products in this Michaelis-Menten model only asymptotes when the system approaches substrate exhaustion. If it is a valid assumption that anaerobic VFA uptake exhibits "Michaelis-Menten like behavior," then the shape of the observed anaerobic phosphate release suggests that the VFA is quickly being exhausted in the first half of the anaerobic RAS reactor. This suggests that the volume and footprint of the anaerobic RAS reactor are sufficiently sized to facilitate proper anaerobic VFA uptake. Also, greater than 95% of the APRR occurs in the first half the anaerobic RAS reactor in all of the anaerobic phosphate release profiles collected.

Further work needs to be conducted on the anaerobic RAS reactor to determine the maximum APRR capacity that one anaerobic RAS reactor can produce. If the novel EBPR configuration becomes a permanent process, it will be important to understand how APRR will be affected when one of the anaerobic RAS reactors is taken out of service for routine maintenance. Currently, the anaerobic RAS reactors are sufficiently sized for anaerobic VFA uptake and the data suggests that the overwhelming majority of the APRR happens in the first half of the reactors. Further research involving the sizing of the anaerobic RAS reactors should focus on attempting to answer the questions below.

- Is it possible that the anaerobic volume could be reduced even further and still produce sufficient APRR?
- What ratio of RAS flow to GTO flow will optimize the APRR?
- Can the volume of the anaerobic RAS reactor be further reduced by increasing the RAS solids concentrations in the reactor?

APRR

The APRR measure takes into account the RAS throughput and the availability of VFA. The APRR has varied from approximately 1200 kg-P/day to a maximum of approximately 2200 kg-P/day. When the APRR increases the downstream aerobic phosphate uptake capacity increases. Likewise, when the APRR decrease the observed phosphate uptake capacity decreases. The data trend predicts that the mass of phosphate removed in the downstream aeration basin is approximately 2 times the mass of the APRR. For example, if the APRR equals 2000 kg-P/d, then approximately 6000 kg-P/d of phosphate will be removed in the aeration basin. Operation of the EBPR configuration should strive to maximize the APRR to produce the best phosphate removal. One limitation associated with the APRR is that the APRR can only be accurately calculated with grab sample data and the actual range of diurnal variation is not known because all the grab sample data set have been collected once per day during the daylight periods of the days. The loading and flows to the plants in vary hourly and the impact of diurnal load variation is not known on the overall APRR. The relationship between ultimate daily phosphate removal capacity and the diurnal variability of APRR needs to be further explored.

If online phosphate probes were installed in the RAS, GTO and anaerobic RAS reactor effluent, then a simple real-time APRR calculation could easily be developed using a mass balance approach. A real-time APRR calculator would be beneficial is immediately identifying anaerobic RAS reactor process upsets and would be crucial in developing and understanding how upstream operational changes to gravity thickener,

RAS and GTO influence the APRR and this information would allow further optimization of the EBPR configuration. Also an online APRR calculator would allow the collection of a dataset that could develop long-term relationships between effluent phosphate concentrations and APRR.

The APRR fraction is a measurement of the balance between phosphate loading and phosphate uptake capacity in the aeration basins. The data shows that when the APRR fraction is 30% or more of the phosphate load to the downstream MLE aeration basins, the effluent phosphate concentrations are ultra-low. If an online APRR calculator was developed then it would be very easy to develop an online APRR fraction calculator. A real-time APRR fraction calculator would be the best operational control strategy to reliable and consistently produce low effluent phosphate concentrations. A simple control loop could be implemented that could control acetic acid fed to the anaerobic RAS reactor or increase GTO flows rates in an effort to increase APRR during peaking events or during times when the carbon loading in the GTO is insufficient to produce the required APRR. The APRR fraction is a simple calculation and the best predictor of effluent phosphate concentrations. It was determined that NSEC final effluent phosphate concentrations is not the most accurate way to evaluate the performance of the phosphate removal from the EBPR configuration because there were large fluctuations in phosphate loading from upstream phosphate sources. The APRR fraction calculator solves that dilemma.

Anaerobic SRT and effluent phosphate concentrations

The anaerobic SRT was calculated as the mass of MLSS in the anaerobic RAS reactor divided by the total solids wasting from the NSEC. The anaerobic SRT

calculation is highly influenced by the RAS TSS concentration, the ratio of GTO to RAS flows going to the anaerobic RAS reactor and the NSEC sludge wasting rate.

There is no apparent correlation between anaerobic SRT and aerobic uptake rate, note that for any given anaerobic SRT there is a large variation in the observed aerobic uptake. For example, an anaerobic SRT of 0.40 days shows a range of aerobic uptake of 3150 – 5600 kg-P/d. This is a large range of variation and suggests that anaerobic SRT is not a useful measure in the prediction of downstream aerobic uptake rates.

There is no clear correlation between anaerobic SRT and aeration basin effluent phosphate concentration, note that for any given anaerobic SRT there is a large variation in the aeration basin effluent phosphate concentration. For example, an aeration basin effluent phosphate concentration of less than 0.5 mg-P/L occurs at an aerobic SRT as low as 0.35 days all the way to an SRT of 0.45 days. This is a large range of variation and suggests that anaerobic SRT is not a useful measure in the prediction of aeration basin effluent phosphate concentrations

Aerobic uptake

There is a trend that high aerobic phosphate uptake rates produces lower effluent phosphate concentrations but the aerobic uptake rate does not take into account the phosphate loading to the aeration basin. For example, the lowest aerobic phosphate uptake rate observed, 2500 kg-P/d, produced an aeration basin effluent phosphate concentration of 0.03 mg-P/L. This happened because the phosphate loading to the aeration was only 2500 kg-P/L that day and entire NSEC and EBPR complex was being operated under a phosphate limited situation. It is likely that the observed aerobic phosphate rate would have been higher during this day but there was no more phosphate

in the bulk liquid to take and observed phosphate uptake rate can't exceed the phosphate loading to the aeration basin.

CHAPTER VII

RAS Fermentation

Introduction

RAS fermentation is a concept tested during phase IV of the study between April 1st and April 16th 2012. The basis of the RAS fermentation concept is that we would stop conveying GTO to the anaerobic RAS reactor and endogenous decay and fermentation of secondary sludge (RAS) would supply the carbon to the PAOs to satisfy the anaerobic VFA uptake requirement of EBPR. There were two variation of RAS fermentation testing phase. First RAS fermentation was tested with the anaerobic RAS reactor mixers on in normal operation and during the second test period of RAS fermentation the mixers in the anaerobic RAS reactor would be shutoff. During the RAS fermentation testing period with the mixers off, the first three mixers in the anaerobic RAS reactor would be shutoff for twenty three and half hours per day and pulsed on for thirty minutes each day to prevent excessive sludge from accumulating in the anaerobic RAS reactor.

Methodology

Extensive phosphate profiling was conducted in the anaerobic RAS reactor and in the downstream aeration basins. The anaerobic phosphate release and aerobic phosphate uptake profiles will be examined. Influent and effluent phosphate concentrations will be monitored, as well as TSS in the anaerobic RAS reactor. The laboratory analysis was conducted by Technical Service Laboratory according to standard methods.

Results

Two phosphate profiles were conducted during the RAS fermentation period. The observed anaerobic phosphate release in the anaerobic RAS reactor was 480 and 510 kg-P/d. See figure 28, below, for the observed anaerobic phosphate release profile.

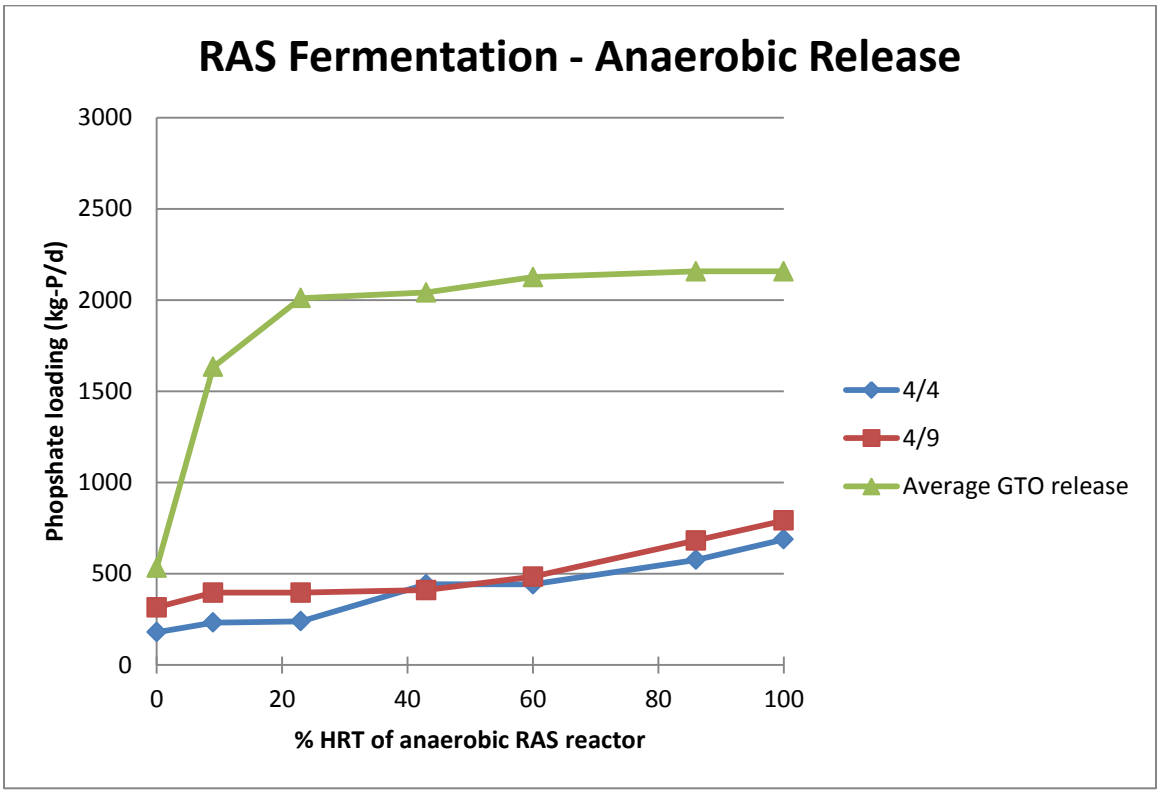

Figure 27. Observed anaerobic phosphate release profile during RAS fermentation test period.

The coupled aerobic phosphate uptake profile is below, in figure 29.

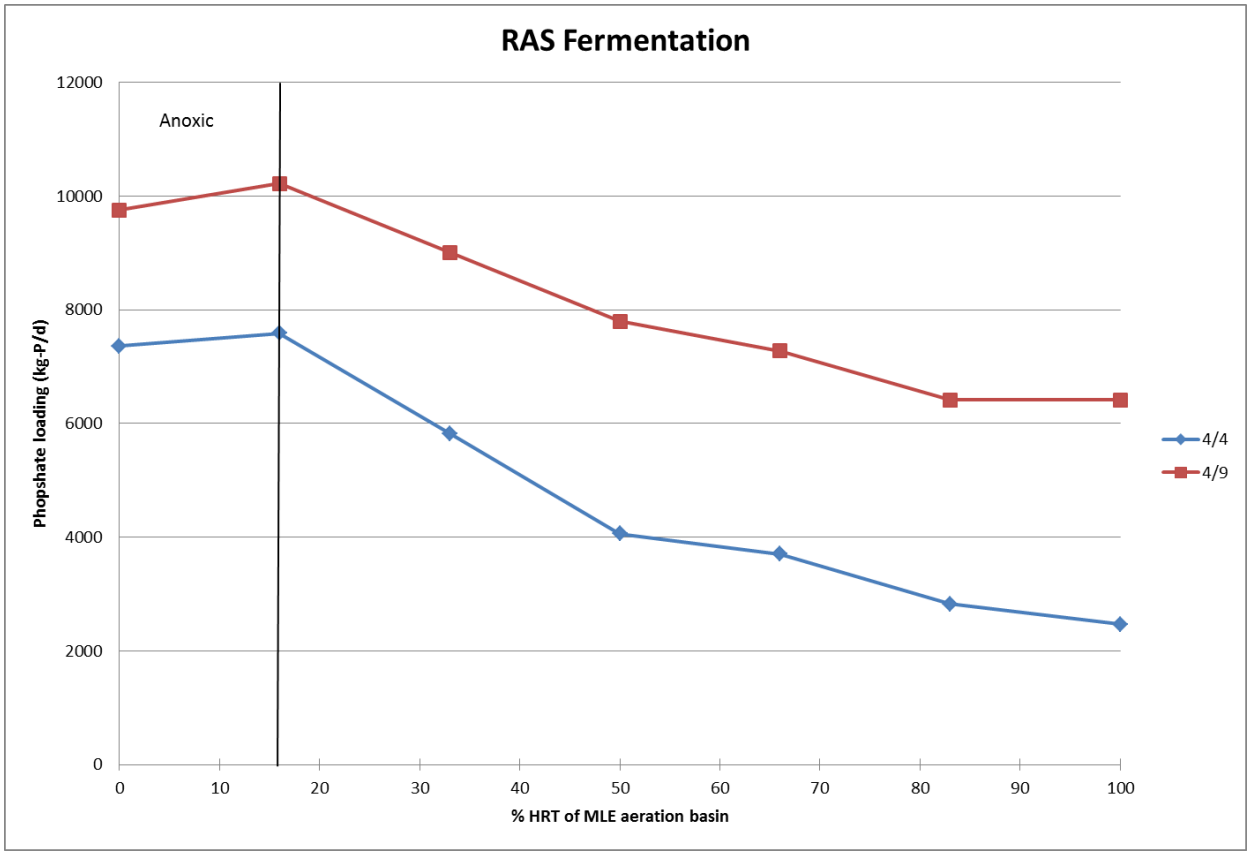

Figure 28. Aerobic phosphate uptake profile during RAS fermentation stage of study.

The average effluent phosphate profile during RAS fermentation was 2.14 mg-P/L and the average observed phosphate uptake was 3700 kg-P/d. The solids profiling results show significant solids stratification and accumulation in the anaerobic RAS reactor with the mixers shutoff, figure 30 below.

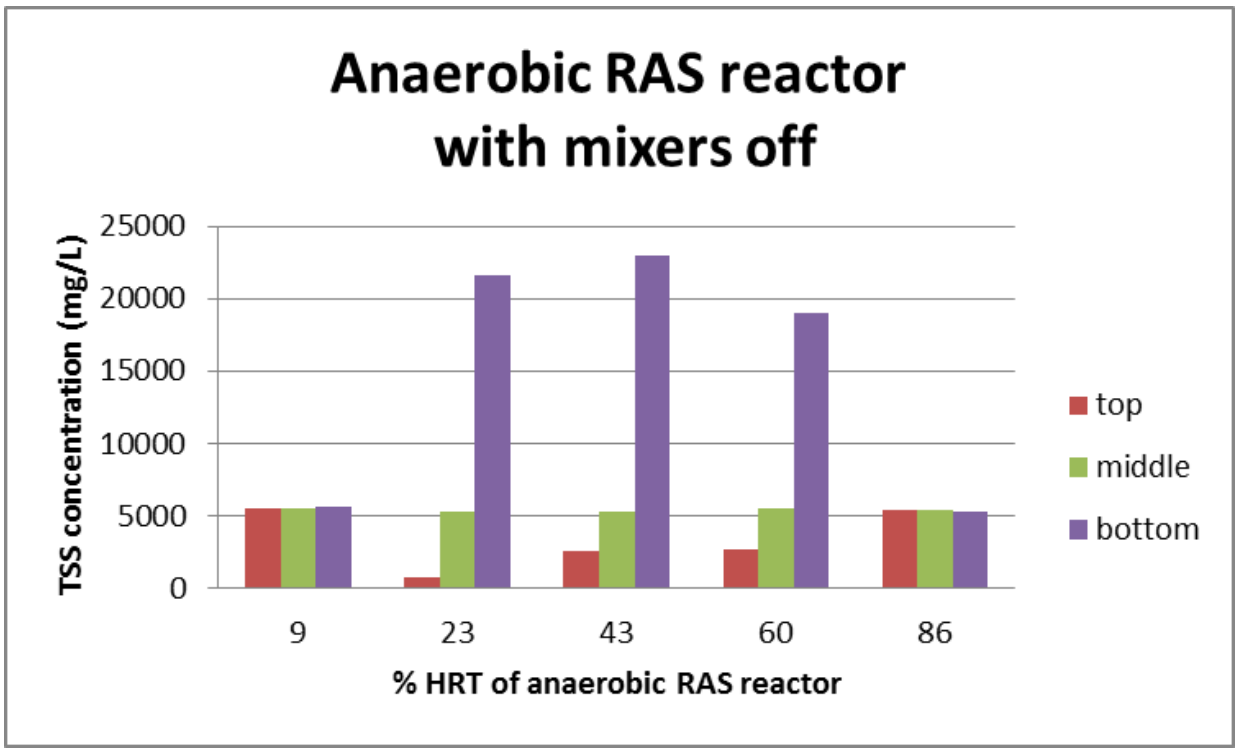

Figure 29. Solids profile of anaerobic RAS reactor with mixers off.

When the mixers in the anaerobic RAS reactor are pulsed on for 30 minutes the settled solids become suspended, see figure 31 below.

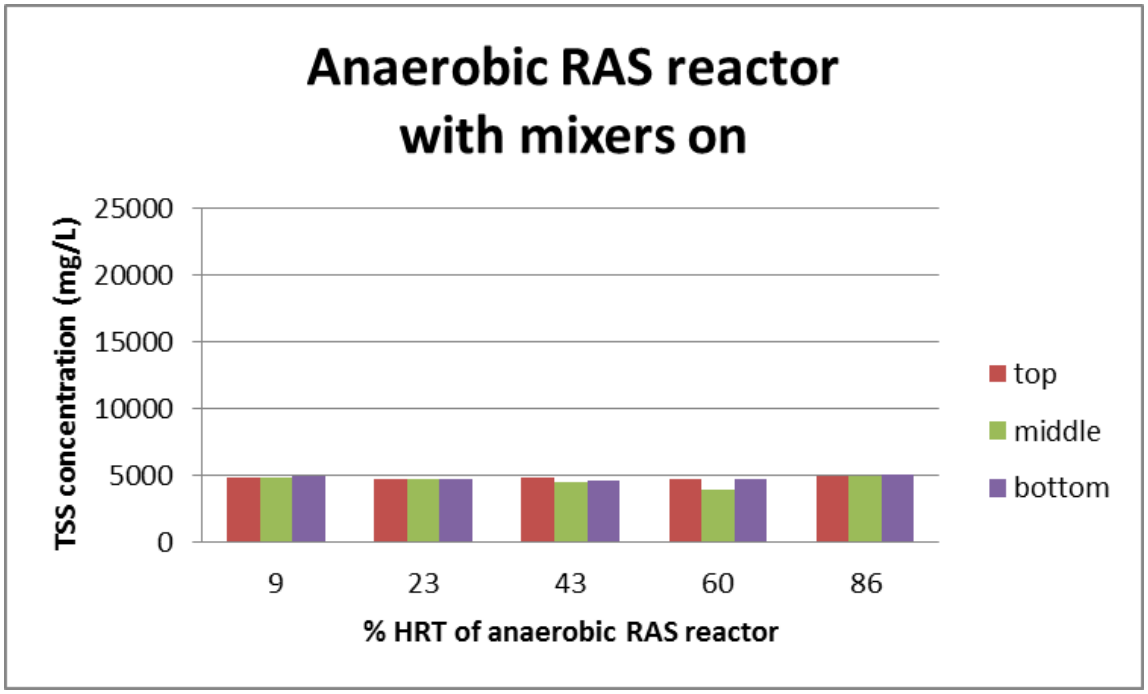

Figure 30. Solids profile with mixers turned on in anaerobic RAS reactor.

The solids accumulation on the floor of the anaerobic reactor is eliminated when the mixers are turned on. Also note that relatively homogenous solids concentrations are observed with the mixers on.

Conclusion

RAS fermentation is not a feasible operation strategy for the novel side stream EBPR process to provide sufficient VFA in the anaerobic zone. Whether the mixers are on or off, the observed anaerobic phosphate release is less than 25% of the anaerobic phosphate release observed when GTO is the carbon source. The most telling evidence that RAS fermentation is not a viable option to supply sufficient VFA is that the aerobic uptake is about 35% less than the average aerobic uptake observed during EBPR operation with GTO being conveyed to the anaerobic RAS reactor. Also the average

effluent phosphate concentration is 2.14 mg-P/L, which is just slightly less than the historical effluent average of 2.40 mg-P/L.

CHAPTER VIII

Engineering Significance and Final Conclusions

The side stream EBPR configuration shows advantage over mainstream EBPR configuration because the anaerobic conditions in the side stream anaerobic RAS reactor are protected from electron acceptors. Both nitrate from de-nitrification and oxygen from back mixing are not important in the side stream configuration. Another advantage of side stream design is that small footprints of the anaerobic zone are possible because the MLSS concentrations are very high in the anaerobic RAS reactor because the RAS is concentrated in the final clarifiers before it is conveyed to the anaerobic RAS reactor. The high MLSS concentration inherently allows the reaction rates to be higher and because of this, the high solids concentration also allows for a very rapid uptake of VFA once it becomes available in the anaerobic zone.

In relation to other WWTP retrofitting EBPR configurations, this side stream EBPR approach is appealing because it can be implemented with minimal modification to existing nitrification/de-nitrification processes. As long as RAS flows and a carbon source can be directed to a side stream reactor, the EBPR configuration can simply be added to existing processes without hindering existing nitrogen removal capacity. This is good because it reduces construction cost associated with replacing existing capacity that was lost due to a retrofitting EBPR. Not only can it be added but the footprint and retrofit cost is relative small compared to conventional mainstream EBPR configuration. Even if an internal carbon source is not available for the side stream anaerobic reactor, external carbon such as acetic acid can easily be used to satisfy the carbon requirement of the side stream reactor.

Conclusions

A short list of conclusions and useful information discovered are listed below:

- When operated correctly the side stream EBPR system is capable of:
  - Ultra low effluent phosphate concentrations
  - Consistent
  - Reliable

- The conventional mainstream EBPR design criteria is not directly applicable

- The pre-study modeling simulations did not predict the level of removal observed

- The EBPR configuration is not adversely affected by poly-aluminum chloride (PAX) dosing to control filamentous organisms. The PAX will precipitate a small portion of the influent phosphate

- The RAS flow rates from the final clarifiers are sufficient enough to prevent excessive secondary phosphate release in the final clarifiers.

- Secondary phosphate release in the final clarifiers is minimal and future EBPR optimization efforts would be most efficient if focused on other EBPR process considerations.

- Operation of the anoxic zone in the MLE aeration basins should focus on nitrogen removal considerations and not phosphate removal.

- RAS fermentation does not support EBPR as a sole carbon source.

- Increased ferric chloride addition to the centrate return flow is an operational control strategy that will reduce phosphate loading to the aeration basins.

- APRR should be maximized to facilitate optimal phosphate uptake capacity and APRR is the most accurate predictor of downstream phosphate uptake capacity.

- Minimum anaerobic SRT design criteria used in conventional EBPR design is not directly applicable to side stream EBPR configurations and anaerobic SRT does not accurately predict aerobic phosphate uptake capacity or effluent phosphate concentrations.

- The APRR fraction is the most accurate predictor of effluent phosphate concentrations and the minimum APRR fraction required to consistently produce ultra-low effluent phosphate concentrations is 30%.

- By installing online phosphate probes in the GTO, RAS, anaerobic RAS reactor effluent, main influent channel and aeration basin effluent it would be possible to

develop simple and easy real-time APRR calculators and real-time APRR fraction calculators.

- Blanket depths in gravity thickener are important to carbon concentration in GTO
- The RAS suspended solids concentrations are important to maintain anaerobic throughput and anaerobic mass fraction
- Novel EBPR configuration capable of excellent phosphate removal with less than half the carbon loading required by conventional design criteria
- The anaerobic RAS reactor is sufficiently sized to support APRR and possibility could be even further reduced in size
- Further work is needed to optimize the novel EBPR configuration
- The side stream EBPR configuration shows advantage over conventional design and is being considered in next facility plan

Further work needed

If the gravity thickener is going to be used as the sole carbon source to support EBPR, then further work needs to be done to optimize the VFA loading in the GTO. There are large potential economic benefits that can be realized if the operation of the gravity thickener is optimized. The estimated annual cost of acetic acid is between 1.6 and 3.2 million dollars a year, which can be avoided if the gravity thickener operation is optimized. Testing of an elutriation loop in the gravity thickener at a higher rate and testing of more advanced blanket control strategies are areas of focus that could assist in optimization efforts.

Examination and investigation of strategies that reduce phosphate loading to the aerations basins is another area of potential work that could assist in optimizing the side stream EBPR configuration. It became apparent that the balance between phosphate loading and removal capacity has a huge influence on EBPR performance and effluent

phosphate concentrations. Further EBPR process optimization could be realized by implementing new technologies or control strategies that reduce phosphate loading to the aeration basins. One example of an emerging technology that could accomplish this would be implementation Ostara or another similar phosphorus recovery technology to the centrate return stream. A phosphorus removal technology would not only assist in EBPR process optimization but it would also be a more sustainable approach. Another similar strategy that needs further evaluation in would be development and investigation of a control loop that controlled ferric chloride dosing to the centrate return based on phosphate concentration in the centrate stream.

Finally, it is apparent that better instrumentation is needed in the NSEC to optimize the EBPR configuration. Online phosphate probes are needed in the RAS, centrate, main influent channel, aeration basin effluent and GTO streams. Addition of these probes would allow the development of real time APRR and APRR fraction calculators. The data from the study shows that APRR fraction is the best predictor of effluent phosphate concentrations and this could be a great EBPR operational parameter to use in the further optimization efforts. The online phosphate probes would also allow a better understanding of the EBPR process by learning of a cause and effect relationship. Currently, there are no reliable online phosphate probes in the NSEC and this presented a challenge during the full-scale study because MWRD staff didn't have any phosphate data at a high enough temporal resolution to clearly see any cause and effect relationships from process modifications or changes. Outside of the phosphate grab sampling efforts, the only phosphate data we collected was daily composite samples. The daily composite samples made it impossible to determine how the EBPR process varied at time intervals

of less than one day and the grab sampling efforts only allowed a snapshot of process conditions.

Bibliography

Ahn Y.H. and Speece R.E., 2006. Elutriated acids fermentation of municipal primary sludge. *Water Research*. 40, 2210-2220.

American Public Health Association, 1998. *Standard Methods for Examination of Water and Wastewater*. 20th edition. American Public Health Association/American Water Works Association/Water Environment Federation, Washington DC, USA.

Barker, P.S. and Dold. P.L., 1997. General model for biological nutrient removal activated-sludge systems: model presentation. *Water Environment Research.* 69, 969-984.

Barnard, J.L., 1984. Activated Primary Tanks for Phosphate Removal. *Water SA.* 10(3): 121-126.

Barnard J., Houweling D., Analla H., and Steichen M., 2010. Fermentation of mixed liquor for phosphorus removal. WEFTEC 2010. 59-71.

Bell M., Netto H., Haug R.T., Redd K., Hammond S., and Hartnett W., 2010. Nutrient Removal Practise Implemented at the City of Los Angeles Upstream Water Reclamation Plants. *WEFTEC 2010*. 4455 – 4477.

Blackall L.L., Crocetti G.R., Saunders A.M. and Bond P.L., 2002. A review and update of the microbiology of enhanced biological phosphorus removal in wastewater treatment plants. *Antonie van Leeuwenhoek.* 81, 681-691.

Bouzas A., Ribes J., Ferrer J., Seco A., 2007. Fermentation and elutriation of primary sludge: Effect of SRT on process performance. *Water Research*. 41, 747-756.

Cavanaugh L., Carson K., Lynch C., Phillips H., Barnard J., and McQuarrie J., 2012. A Small Footprint Approach for Enhanced Biological Phosphorus Removal: Results froma 106 mgd Full-scale Demonstration. *In Proceeding of WEFTEC 2012 conference.*

Chanona J., Ribes J., and Ferrer J., 2006. Optimum design and operation of primary sludge fermentation schemes for volatile fatty acid production. *Water Research.* 40, 53-60.

Comeau, Y., Oldham W.K., and Hall K.J., 1987. Dynamics of carbon reserves in biological dephosphatation of wastewater. In *Proceedings of an International Association on Water Pollution Research and Control on Biological Phosphate Removal from Wastewaters,* ed. R. Ramadori, 39-55. Oxford: Pergamon Press.

Eastman J.A. and Ferguson J.F., 1981. Solubilization of particulate organic carbon during the acid phase of anaerobic digestion. *Water Pollution Control Federation*. 53 (3), 352-366.

Elefsiniotis, P. and W.K. Oldham. 1991. The effect of operational parameters on the acid-phase anaerobic fermentation in the biological phosphorus removal process. In *Proceedings of the ASCE Environmental Engineering Division, National Conference on Environmental Engineering,*Reno, NV, 325-330. New York: American Society of Civil Engineers.

Fuhs, G.W. and M. Chen. 1975. Microbiological Basis of Phosphate Removal in the Activated Sludge Process for the Treatment of Wastewater. *Microbial Ecology*. 2(2): 119-38.

GonCalves, R.F., Charlier A.C., and Sammut F., 1994. Primary fermentation of soluble and particulate organic matter for wastewater treatment. *Water Science and Technology* 30(6): 53- 62.

Henze, M., Gujer, W., Mino T., Wentzel, M., Marais, G., and Lossdrecht, M., 1999. Activated sludge model No. 2D, ASM2D. *Water Science Technology* 39 (1): 165-182

Himmi E.H., Bories A., Boussaid A., and Hassani L., 2000. Propionic acid fermentation of glycerol and glucose by *Propionibacterium acidipropionic* and *Propionibaterium freudenreichii* ssp. *Shermanii*. Applied Microbiology and Biotechnology. 53 (4), 435-440.

Houweling D., Dold P., and Barnard J., 2010. Theoretical Limits to biological phosphorus removal: Rethinking the influent COD:N:P ratio. WEFTEC 2010. 7044-7059.

Knowles J.R., 1980. "Enzyme-catalyzed phosphoryl transfer reactions". *Annual Review of Biochemistry*. 49: 877–919

Lie, E. and Welander T., 1997. A method for determination of the readily fermentable organic fraction in municipal wastewater. *Water Research 31(6): 1269-1274*

Neethling, J.B., Bakke B., Benisch M., A. Gu, Stephens H., Stensel H.D., and Moore R., 2005. Factors Influencing the Reliability of Enhanced Biological Phosphorus Removal. Alexandria, VA: *WERF and IWA Publishing*.

Oehmen A., Saunders A.M., Vives M.T., Yuan Z., and Keller J., 2005. Competition between polyphosphate and glycogen accumulating organisms in enhanced biological phosphorus removal systems with acetate and propionate as carbon sources. *Journal of Biotechnology*. 123, 22-32.

Oehmen A., Lemos P.C., Carvalho G., Yuan Z., Keller J., Blackall L. L., and Reis M.A.M., 2007. Advances in enhanced biological phosphorus removal: From micro to macro scale. *Water Research*. 41, 2271-2300.

Pasztor I., Thury P., and Pulai J., 2009. Chemical oxygen demand fractions of municipal wastewater for modeling of wastewater treatment. *International Journal of Environmental Science Technology*. 6, 51-56.

Randall, C. W. and R. W. Chapin. 1997. Acetic Acid Inhibition of Biological Phosphorus Removal. *Water Environment Research*. 69(5):955-960.

Rossle W.H. and Pretorius W.A., 2001. A review of characterization requirements for in-line prefermenters Paper 1: Wastewater characterization. *Water SA*. 27 (3) 405 – 412.

Skalsky D.S., and Daigger G.T. 1995. Wastewater solids fermentation for volatile acid production and enhanced biological phosphorus removal. *Water Environment Research* 67(2): 230-237.

Temmink, H., Petersen B., Isaacs S., and Henze M., 1996. Recovery of biological phosphorus removal after periods of low organic loading. *Water Science and Technology* 34(1-2): 1-8.

Thomas, M., Wright, P., Blackall, L., Urbain, V., and Keller, J., 2003. Optimization of Noosa BNR plant to improve performance and reduce operating costs. *Water Science Technology*. 47 (12), 141–148.

Ucisik A.S., and Henze M., 2008. Biological hydrolysis and acidification of sludge under anaerobic conditions: The effect of sludge type and origin on the production and composition of volatile fatty acids. *Water Research*. 42, 3729-3728.

USEPA. 1993. Nitrogen Control Manual. Office of Research and Development. EPA/625/R-93/010. September 1993.

USEPA. 2009. Nutrient Control Design Manual, State of Technology Review Report. Office of Research and Development. EPA/600/R-09/012. January 2009.

WEF and ASCE. 1998. Design of Municipal Wastewater Treatment Plants - MOP 8, 4th Ed. Water Environment Federation and American Society of Civil Engineers. Alexandria, VA: WEF.

WEF and ASCE. 2006. Biological Nutrient Removal (BNR) Operation in Wastewater Treatment Plants -MOP 29. Water Environment Federation and the American Society of Civil Engineers. Alexandria, VA: WEFPress.

Wentzel, M.C., Ekama G.A.,. Lowenthal R.E, Dold P.L., and Marais G.R. 1989. Enhanced polyphosphate organism cultures in activated sludge systems. Part II: Experimental behaviour. *Water SA* 15(2): 71-88.

Yuan Q., Baranowski M., and Oleszkiewicz J.A., 2010. Effect of sludge type on the fermentation products. *Chemosphere*. 80, 445-449.

Yuan Q. and Oleszkiewicz J., 2010. Effect of anaerobic HRT and secondary phosphorus release on enhanced biological phosphorus removal. *WEFTEC 2010*, 7132-7134

Zeng R.J., Loosdrecht M.C.M., Yuan Z.G., and Keller J., 2003. Metabolic model for glycogen-accumulating organisms in anaerobic/aerobic activated sludge systems. *Biotechnology and Bioengineering*. 81 (1), 92-105.

Zeng R.J., Yuan Z., and Keller J., 2006. Effects of solids concentration, pH and carbon addition on the production rate and composition of volatile fatty acids in prefermenters using primary sewage sludge. *Water Science Technology*. 53 (8), 263–269.

Appendix

A. Acronyms

APRR – Anaerobic Phosphate Release Rate
AR – Anaerobic Reactor
BNR – Biological Nutrient Removal
BOD – Biochemical Oxygen Demand
CaRRB – Centrate and Return activated sludge Re-aeration Basin
COD – Chemical Oxygen Demand
EBPR – Enhanced Biological Phosphorus Removal
GTO – Gravity Thickener Overflow
GVT – Gravity Thickener
HRT – Hydraulic Residence Time
MLE – Modified Ludzack-Ettinger treatment process
MLR – Mixed Liquor Return
MWRD – Metro Wastewater Reclamation District
NSEC – North Secondary Treatment Complex
RAS – Return Activated Sludge
rbCOD – Readily Biodegradable Chemical Oxygen Demand
RWHTF – Robert W. Hite Treatment Facility
sbCOD – Slowly Biodegradable Chemical Oxygen Demand
SRT – Solids Residence Time
SSEC – South Secondary Treatment Complex
TSS – Total Suspended Solids
VSS – Volatile Suspended Solids
VFA – Volatile Fatty Acid
WAS – Waste Activated Sludge

B. rbCOD determination using ffCOD method

Aerated ffCOD method - rbCOD determination

rbCOD concentration of the GTO can be estimated by aerating a mixture of GTO and RAS. The rbCOD in the GTO will be consumed during the aeration and the deficit between the initial calculated ffCOD and measured aerated ffCOD will be the amount of rbCOD lost. The deficit can then be used to calculate the rbCOD concentration in the GTO sample. The volume and ffCOD concentration must be known for RAS, GTO and RAS/GTO mixture.

Determining rbCOD from ffCOD

Given: V_{ras} = RAS volume
V_{gto} = GTO volume
C_{ras} = RAS ffCOD concentration
C_{gto} = GTO ffCOD concentration
C_{mix} = ffCOD concentration of mixture of RAS/GTO that has been aerated for ≥4hrs

Problem: Calculate the rbCOD concentration of GTO ($C_{rbCOD,\ gto}$)

Assumptions:

1) RAS has an rbCOD concentration of zero
2) All the rbCOD has been consumed during the aeration period of the mixture

$$\boldsymbol{C}_{ras}\boldsymbol{V}_{ras} + \boldsymbol{C}_{gto}\boldsymbol{V}_{gto} = \boldsymbol{C}_{T,initial}\,(\boldsymbol{V}_{ras} + \boldsymbol{V}_{gto}) \quad (1)$$

$$\boldsymbol{C}_{T,initial} - \boldsymbol{C}_{mix} = \boldsymbol{C}_{deficit} \quad (2)$$

$$\boldsymbol{C}_{rbCOD,\ gto} = \boldsymbol{C}_{deficit}\,(\boldsymbol{V}_{ras} + \boldsymbol{V}_{gto}) / \boldsymbol{V}_{gto} \quad (3)$$

rbCOD calculation:

V_{ras} = 1.30 L
V_{gto} = 0.76 L
C_{ras} = 42.0 mg/L
C_{gto} = 195.5 mg/L
C_{mix} = 52.0 mg/L

$$\frac{(42mg/L)(1.3L) + (195.5mg/L)(0.76L)}{2.06L} = 98.6mg/L = C_{T,initial} \quad (1)$$

$$98.6\ mg/L - 52\ mg/L = 46.6\ mg/L = C_{def} \quad (2)$$

$$\frac{(46.6mg/L)(2.06L)}{0.76L} = 126.3mg/L = C_{rbCOD,gto} \quad (3)$$

$C_{rbCOD,\ gto}$ = 126.3 mg/L